



Numerical Analysis of Behavior of Corbels Strengthened with Carbon Fiber-Reinforced Polymer

Hiba Zaioune¹ · Samy Mezhoud¹

Received: 30 July 2022 / Accepted: 1 February 2023 / Published online: 17 February 2023
© The Author(s), under exclusive licence to Shiraz University 2023

Abstract

Reinforced concrete corbels in precast structures are the most popular type of connection between beams and columns. Nonetheless, corbels collapse in most cases in a catastrophic and sudden way due to a variety of factors. Despite the fact that numerous studies have been conducted to strengthen the damaged concrete elements with external reinforcement techniques, there are only a few studies have been conducted specifically to investigate the effects of external reinforcement by fiber-reinforced polymer on the shear response. The present paper aims to simulate the nonlinear structural behavior of reinforced concrete corbels externally strengthened with carbon fiber-reinforced polymer strips. Therefore, a case study of corbel was chosen in order to elaborate a several three-dimensional finite element models by varying in amount, direction, and thickness of the carbon strips. The reliability of the numerical models was validated by comparing the numerical results to the data of experimental campaign of previous published studies. The validated model was then used in a parametric study to investigate the major parameters that significantly influence corbel behavior, such as the influence of the compressive strength of concrete and the effect of the secondary reinforcements. The results showed that the diagonal reinforcement limited shear crack propagation and widening, resulting in a gain in load capacity of up to 66%. In addition, the increase of the ratio of shear span-to-effective depth a/d from 0.5 to 1.0 decreased load capacity by up to 40%, which confirmed that the corbel strength is much affected by increasing span–depth ratio. Moreover, the thickness of the carbon strips has more effect on the ultimate load, ductility, and toughness of the corbels, especially in inclined configuration resulting in an increase in shear capacity up to 123%. The increase in the compressive strength of concrete leads to improve the shear capacity by up to 57%. Furthermore, the incorporation of horizontal secondary reinforcement contributed along the depth of the corbels to an additional strength gain of up to 16%. The numerical behavior results are rather well-matched to those found experimentally in the term of load–deflection curves.

Keywords Reinforced concrete · Corbel · Strengthening · CFRP strips · Shear strength · Thickness · Secondary reinforcement

1 Introduction

Over the past few decades, precast-reinforced concrete elements have become increasingly often used in the construction of buildings and bridges. Corbels are the most common type of connectors used in the design of precast structural

systems because of their key benefits of ease of connection, speed during construction, and cheaper construction costs (Strauss et al. 2006; Canha et al. 2014; ARAÚJO et al. 2017; Gulsan et al. 2021). Corbels are short cantilever elements that extend from the interior face of columns or walls and are used to transfer vertical and horizontal loads from beams to walls or columns. They are frequently employed in reinforced concrete (RC) parking garages, precast structures, and industrial buildings. They are distinguished by a shear span-to-depth ratio less than one and a complicated flow of internal stresses (Jawad and Abdul-Hasan 2018; El-Maaddawy and Sherif 2014; Ridha et al. 2017; ACI318 2019).

Corbels are similar to other structural-reinforced concrete elements, they are susceptible to a variety of factors that

✉ Hiba Zaioune
hiba.zaioune@umc.edu.dz

✉ Samy Mezhoud
mezhoud.sami@umc.edu.dz

¹ Laboratory of Materials and Construction Durability (LMDC), Civil Engineering Departement, University of Constantine 1, Constantine, Algeria

lead to degradation, such as steel corrosion. This problem is the root cause of several diseases in reinforced concrete structures exposed to extreme climatic conditions and high temperatures seen in industrial structures. As a result, the shear strength of corbels may be decreased and they may fail in a brittle way, resulting in the catastrophic destruction of the building. For this reason, RC corbels need to be strengthened or repaired more as a result of these significant deteriorations. Corbel damage can also occur for a number of other causes, such as excessive loads, cracks brought on by high vibration, structural fatigue, construction or design errors, and code revisions (Ivanova et al. 2019; Abdulhaleem et al. 2018; Abu-Obaida et al. 2020; Jafarian et al. 2020). The main modes of failure of RC corbel can occur by bending, concrete crushing on the strut, shear at the interface between the corbel and the column, loss of anchorage of the main tie reinforcement, and concrete crushing under the bearing plate (ARAÚJO et al. 2017).

Several previous studies focused on the experimental and analytical examination to identify the variables that influence the structural behavior of RC corbels when subjected to vertical and horizontal forces. The most reported variables are: shear span-to-depth ratio, the shape, the dimension of corbels, the type and percentage of longitudinal and transverse steel reinforcements, the strength of concrete, and the use of fibers (Jawad and Abdul-Hasan 2018; Mattock et al. 1976; Fattuhi 1994; Campione 2009; Mohammed et al. 2012; Canha et al. 2014; Campione and Cannella 2020; Yun et al. 2021).

Numerous other studies investigated the potential effects of adding steel fiber reinforced (SFR) to concrete corbels. It was discovered that steel fibers may be employed as secondary reinforcement in place of horizontal stirrups to boost corbel strength capacity, reduce crack width, and improve the failure mode to be gradual and controlled (Fattuhi and Hughes 1989; Fattuhi 1990, 1994; Campione et al. 2005; Campione 2009; Abdulhaleem et al. 2018; Saleh et al. 2019; Gulsan et al. 2021). Moreover, results showed that the use of SFR affect the load-carrying capacity and ductility of RC corbels both before and after exposure to elevated temperatures (Abdulhaleem et al. 2018). It was also revealed that steel and polyolefin fiber can improve the cracking loads, and the shape of the steel fiber clearly affects the ultimate load (Saleh et al. 2022). Using fiber-reinforced polymer (FRP) systems for strengthening has received a lot of attention from researchers in the last decade. The major benefits of this technology are lightweight, high tensile capacity features, ease of installation, insensitivity to corrosion, and high durability. Some research focused on bonding or wrapping by carbon fiber-reinforced polymer (CFRP) composite materials to strengthen and repair RC corbels (Ivanova et al. 2015, 2020; Abed Attiya and Mohamad-ali 2012;

El-Maaddawy and Sherif 2014; Ivanova and Assih 2015; Sayhood et al. 2016; Al-Kamaki et al. 2018). The results indicate that external CFRP is a significant and effective technology for strengthening and repairing RC corbels. It can improve the corbel's performance, durability, and shear strength. Additionally, it was discovered that as the quantity of internal steel reinforcement increased, the exterior CFRP composite reinforcement's contribution to the load capacity reduced (El-Maaddawy and Sherif 2014). Furthermore, it was proven that the technique of near-surface mounted carbon fiber reinforcing may increase corbel strength, reduce crack width, and give more ductile failure (Kareem et al. 2018). Some kinds of shear strengthening of corbels include glass fiber-reinforced polymer (GFRP) bars are tested (Abu-Obaida et al. 2020), the primary reinforcement ratio and the quantity of GFRP ply are found to be also key parameters that influence the level of strength improvement (Ozden and Atalay 2011).

In recent years, nonlinear finite element (FE) programs have been used to simulate the majority of structural components as compared to expensive, time-consuming, and material-intensive experimental work. FE analyses have proven to be more accurate and effective than experimental research in determining stress and strain in RC structures (Jafarian et al. 2020; Barour et al. 2022). Some studies (El-Maaddawy and Sherif 2014; Rafati and Razavi 2016; Abdulridha et al. 2018; Abu-Obaida et al. 2020; Gulsan et al. 2021) conducted a numerical simulation to investigate the response of RC corbels, strengthened, or non-strengthened by FRP material. The results have shown that the FE model is capable to capture the nonlinear behavior of the tested corbels with good accuracy in terms of the stress–strain curve, mode of failure, and crack loads.

Although many types of research have been conducted to study the effect of using external composite reinforcement, there is a great lack of studies carried out on the structural response of short RC corbels strengthened by external composite reinforcement. There is also relatively few numerical research on the prediction of performance, crack patterns, and failure modes of RC corbel reinforced with FRP. To fill this gap well, in this paper, a numerical model was developed and proposed to enhance more the understanding of the nonlinear structural response of RC corbels strengthened with CFRP and to properly predict the primary factors that impact their performance.

The FE models were developed to simulate the nonlinear structural response of nine concrete corbel specimens. The proposed FE model was validated based on the selected experimental data (Abed Attiya and Mohamad-ali 2012), in terms of load deflections. Then, 22 numerical FE models were created to conduct a thorough parametric study that compiles all parameters that significantly influence the behavior of RC corbels (the compressive strength of

concrete (f_c), the inclusion of horizontal reinforcement, and the number of CFRP layers). The results are provided in terms of a load–deflection curves and modes of failure.

2 Numerical Modeling

2.1 Test Specimen

The numerical analysis presented in this study is based on previous experimental data (Abed Attiya and Mohamad-ali 2012). The test specimen included a double-sided corbel connected with a short vertical column, as shown in Fig. 1. The column supporting the two corbels was $150\text{ mm} \times 150\text{ mm}$ in cross section and 450 mm long, and each corbel had a total depth of 150 mm at the face of the column and the effective depth of 125 mm. The corbel was of 150 mm breadth and had a cantilever projection length of 200 mm. The column was reinforced with four deformed bars of 12.7 mm diameter and supported with stirrups of 6 mm diameter and a spacing of 125 mm. The corbel part was reinforced with two deformed longitudinal bars of 12.7 mm diameter as the main reinforcement is located at the bottom with an effective cover of 25 mm. The main reinforcement bars were welded with an anchor near the end of each corbel, to provide an additional anchorage, the diameter of anchor bar is similar to the diameter of main reinforcement.

The corbels specimens were tested up to their ultimate load (V_u), with a maximum capacity of 2000 kN, as shown in Fig. 1 (Abed Attiya and Mohamad-ali 2012).

All specimens were tested in an inverted posture, as seen in Fig. 1. Bearing plates of $150\text{ mm} \times 150\text{ mm}$ were employed at the loading point as supports to prevent local crushing of concrete. The vertical load was delivered to the

top of the column, while the corbels were put on two bearing plates. The loads given to the RC corbel were represented by the support reaction 'V'. The position of the support from the column's faces was altered between these values of shear span-to-effective depth ratio a/d : 0.5, 0.70, and 1 (Abed Attiya and Mohamad-ali 2012).

2.2 Element Type

One of the major numerical approaches for addressing mathematical problems in engineering is FE analysis (Jafarian et al. 2020). The ABAQUS 6.14 (Abaqus 2014) software is used in this study to carry out FE modeling to investigate and predict the behavior and load-carrying capacity of the strengthened RC corbels. As presented in Fig. 5, there are three sorts of elements utilized in this study:

- *Concrete*: C3D8R continuum (solid) element, 8-node linear brick, with reduced integration and hourglass control as presented in Fig. 2a. The element is defined by eight nodes and each node of this element has three degrees of freedom. This element is capable of simulating concrete cracking in tension and crushing in compression. The C3D8R element is used also to model the steel-bearing plates that were placed on the top of the column and at the bottom of each corbel's support (Abaqus 2014; Rafati and Razavi 2016; Abdulridha et al. 2018; Demir et al. 2021).
- *Steel reinforcement*: two nodes truss element T3D2 was used to model the steel bars reinforcement with two end nodes, each node has three translation degrees of freedom as shown in Fig. 2b. The behavior of steel was considered as elastic-perfect plastic (Abaqus 2014; Rafati and Razavi 2016; Abdulridha et al. 2018; Demir et al. 2021).

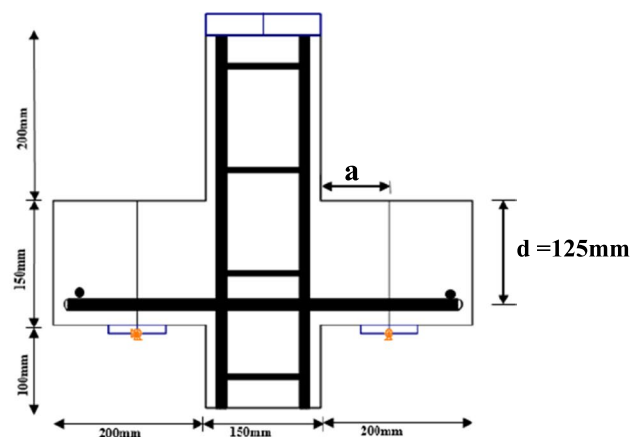
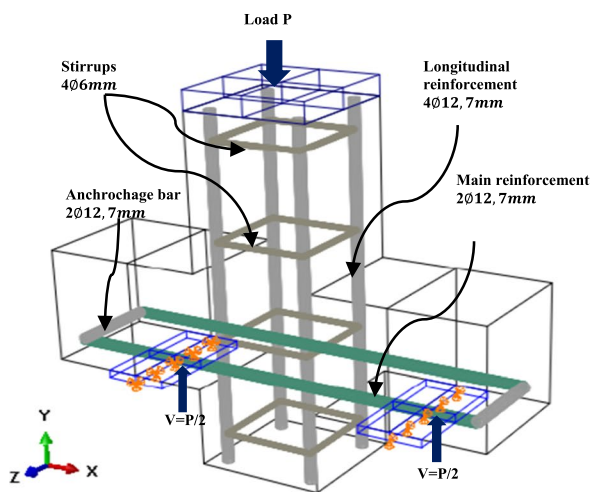
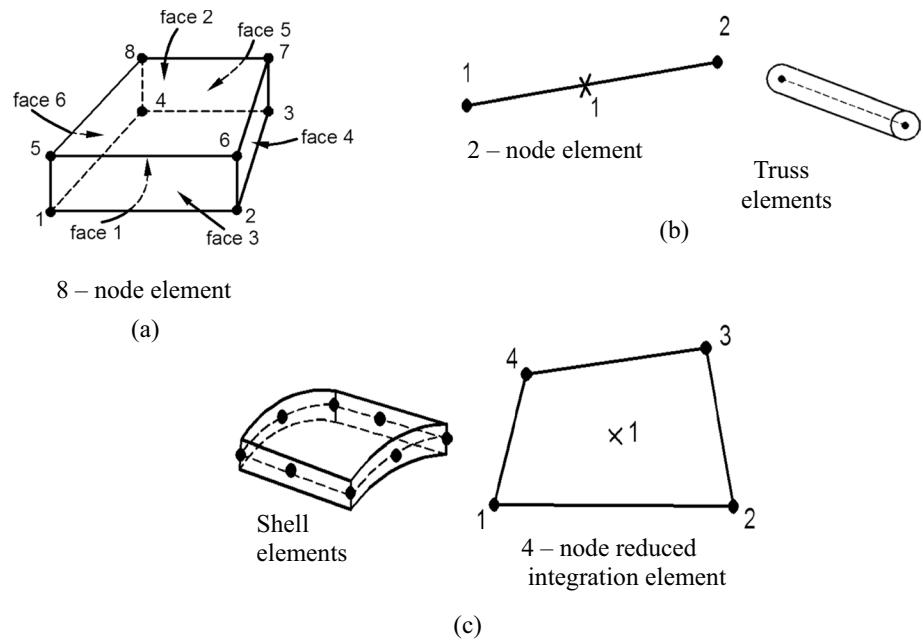


Fig. 1 Dimensions and reinforcement details of simulated test specimen

Fig. 2 Elements type: **a** C3D8R element type, **b** T3D2 element type, **c** S4R element type (Abaqus 2014)



- *Carbon fiber-reinforced polymer (CFRP)*: Four-node shell elements S4R were chosen to model CFRP strips with four nodes and six degrees of freedom in each node. Each node has three translational and rotations translational degrees of freedom, as shown in Fig. 2c. The behavior of CFRP was assumed as linear elastic and the tension strength of the CFRP controlled the rupture (Abaqus 2014; Rafati and Razavi 2016; Abdulridha et al. 2018; Demir et al. 2021).
- Embedded region constraints were selected to embed the reinforcement bars in the concrete column and corbel (host region). The bonding between the steel bar and the concrete was considered to be perfect. In addition, Tie is used to identify the interaction between concrete and CFRP strips (Rafati and Razavi 2016).

2.3 Mesh Sensitivity

A FE mesh sensitivity analysis with three different element sizes was conducted using abaqus. In which, numerical models with various element mesh sizes were created to study the mesh sensitivity in order to figure out the optimal element size using the control specimens CONT1. Elements with mesh sizes of 10 mm (fine mesh), 25 mm (medium mesh), and 60 mm (coarse mesh) were taken into consideration, Fig. 3 displays the RC corbel with three different mesh sizes.

The load–deflection and load–element size behavior for the CONT1 corbel are shown in Fig. 4a, b. The experimental curve and all numerical curves were fairly close. Reducing the mesh size from 60 to 25 mm resulted in a change of 1.34% in results, and when it moved from 25 to 20 mm, the results varied by only 1%, indicating that there was no appreciable variation (Fig. 4b). However, for the following

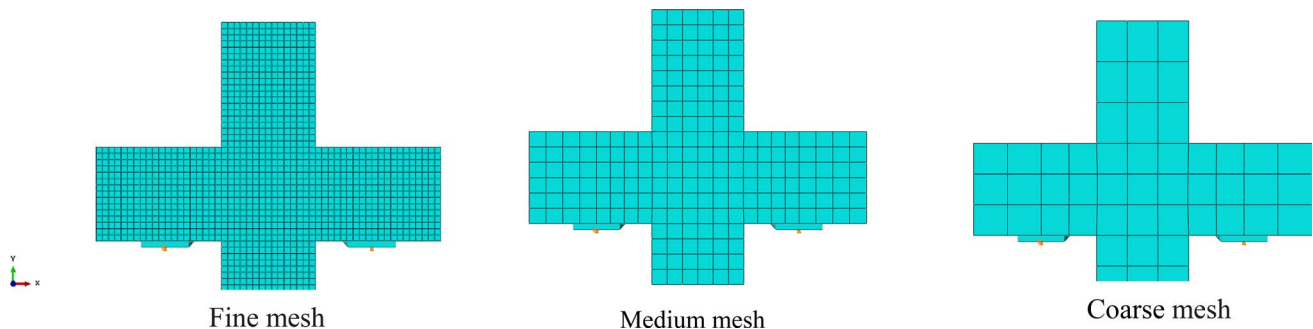


Fig. 3 CONT1 models with three different mesh sizes

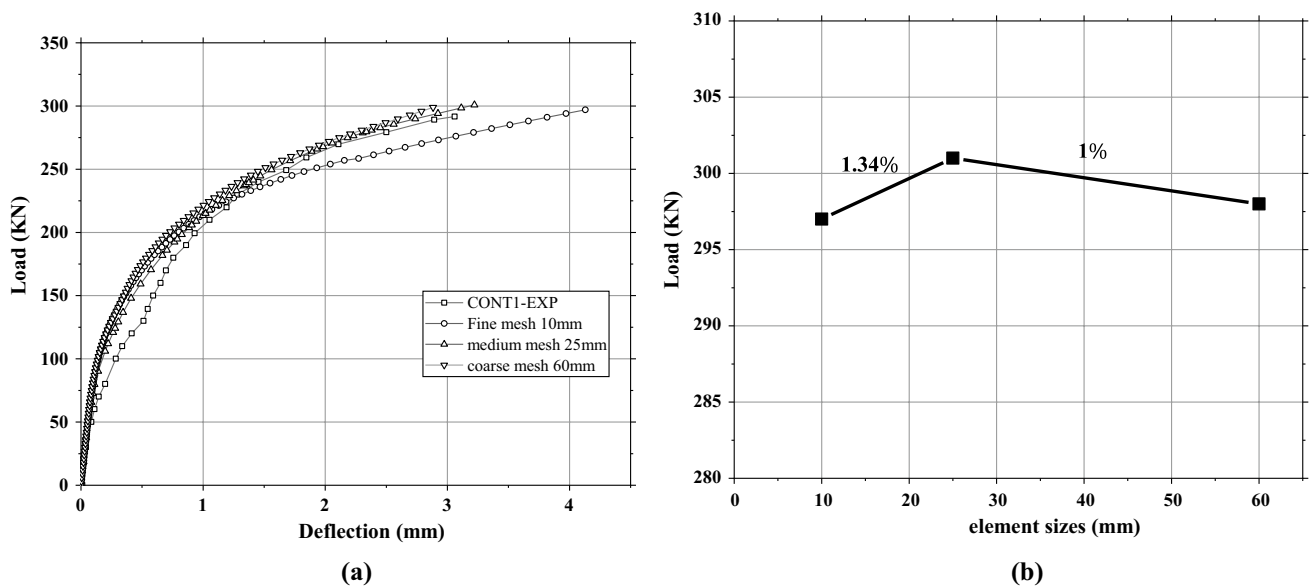
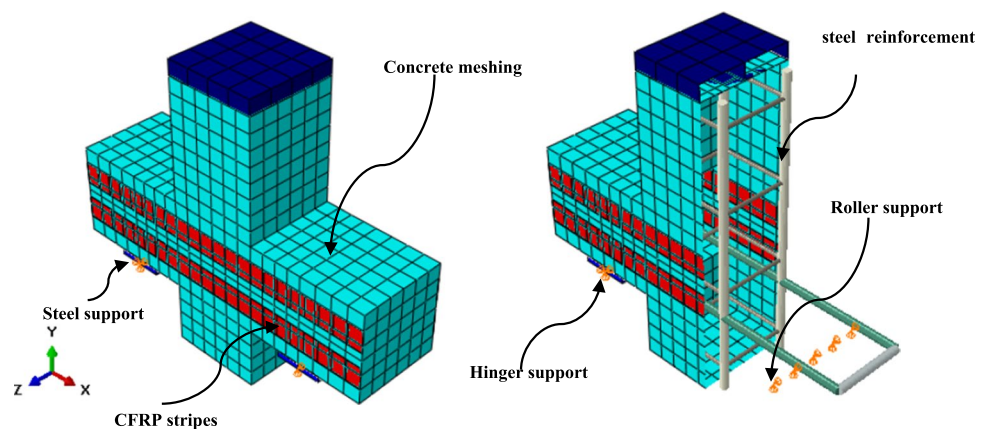


Fig. 4 Effect of element size on the mesh sensitivity: **a** load–deflection curve; **b** load–element size

Fig. 5 Meshing of concrete element, steel reinforcement, and CFRP strips



numerical simulations, a medium-sized mesh of 25×25 mm for the concrete was adopted to create a balance between computing time and accuracy without introducing too many errors. As shown in Fig. 5, 20×20 mm mesh size has been used for steel reinforcing and CFRP strips. Checking the aspect ratio of the numerical model can help guarantee a higher quality mesh, which in turn will provide more precise results. The aspect ratio is the ratio between the longest and shortest edge of an element as described in (Abaqus 2014). Aspect ratios that do not exceed 10 are normally considered to be of high quality; hence, in this study a value of 1.0 was obtained.

2.4 Concrete Damage Plasticity

When using ABAQUS for modeling, it is important to take into account accurate behavioral models for materials. The

selection of behavioral models has a substantial impact on the results, and the conditions must be considered when the model becomes a reality (Rafati and Razavi 2016).

Because concrete has a nonlinear behavior in compression and tension, FE analyses of RC elements are highly complicated. The damage situation in concrete is defined by strain hardening/softening behavior, which is a difficult and intricate process. For this reason, the three crack models: smeared crack concrete model, the brittle crack concrete model, and the concrete damaged plasticity (CDP) model can be used to simulate the damage of RC elements using the ABAQUS program (Wahalathantri et al. 2011).

The concrete damaged plasticity model was chosen from among the three concrete crack models for this investigation. Because it has the capacity to simulate the entire inelastic behavior of concrete in tension and compression, including damage features. As a result, the creation of a

suitable damage simulation model based on the concrete damaged plasticity model will be effective for the analysis of RC structures subjected to a variety of loading conditions, including both static and dynamic loading (Wahathantri et al. 2011).

The CDP constitutive model was based on the equations were given by Lubiner et al. (1989) who proposed a triaxial yield function which was then modified by Lee and Fenves (1998). Lee and Fenves modification took into consideration the different evolution of strength under tension and compression (Athar et al. 2021). The damage plasticity input parameters (inelastic strain, cracking strain, compression damage and tension damage, and other parameters), which were used to represent the nonlinear behavior of concrete are necessary to completely characterize the CDP model. Those numerical values were calculated by using a simplified concrete damage plasticity model based on the equations proposed by (Hafezolghorani et al. 2017). They are shown in Table 1.

• **Uniaxial Compressive Behavior**

The CDP stress–strain relationship in the case of uniaxial compression (Fig. 6b) is represented by a linear branch of the compressive elastic strain, which correlates to the not damaged material ϵ_c^{el} , and a nonlinear branch of the compressive plastic hardening strain, which refers to the damaged material $\epsilon_c^{pl,h}$ (Santos et al. 2020; Jafarian et al. 2020). The plastic hardening strain $\epsilon_c^{pl,h}$ is an important part in determining the relationship between the damage parameters d_c and the compressive strength of concrete σ_c , as given, respectively, by Hafezolghorani et al. (2017) in the following equations:

$$\sigma_c = (1 - d_c)E_0(\epsilon_c - \epsilon_c^{pl,h}) \tag{1}$$

$$\epsilon_c^{in,h} = \epsilon_c - \frac{\sigma_c}{E_0} \tag{2}$$

$$\epsilon_c^{pl,h} = \epsilon_c^{in,h} - \frac{d_c}{1 - d_c} \frac{\sigma_c}{E_0} \tag{3}$$

$$d_c = 1 - \frac{\sigma_c}{\sigma_{cu}} \tag{4}$$

Table 1 Material properties of concrete with CDP model

Concrete compressive behavior		
Stress MPa	Inelastic strain	Damage parameter
21,5	0	0
24	0,000,085	0
28	0,000,234	0
31	0,000,358	0
36	0,000,605	0
40	0,000,885	0
42	0,001,105	0
43	0,001,415	0
42	0,001,725	0,023,255,814
40	0,001,935	0,069,767,442
36	0,002,225	0,162,790,698
31	0,002,465	0,279,069,767
28	0,002,595	0,348,837,209
24	0,002,705	0,441,860,465
21,5	0,002,825	0,5
18	0,002,935	0,581,395,349
16	0,002,995	0,627,906,977
14	0,003,055	0,674,418,605
12,9	0,003,085	0,7
Concrete tensile behavior	Concrete tensile behavior	Concrete tensile behavior
Stress MPa	Stress MPa	Stress MPa
4,3	4,3	4,3
0,043	0,043	0,043

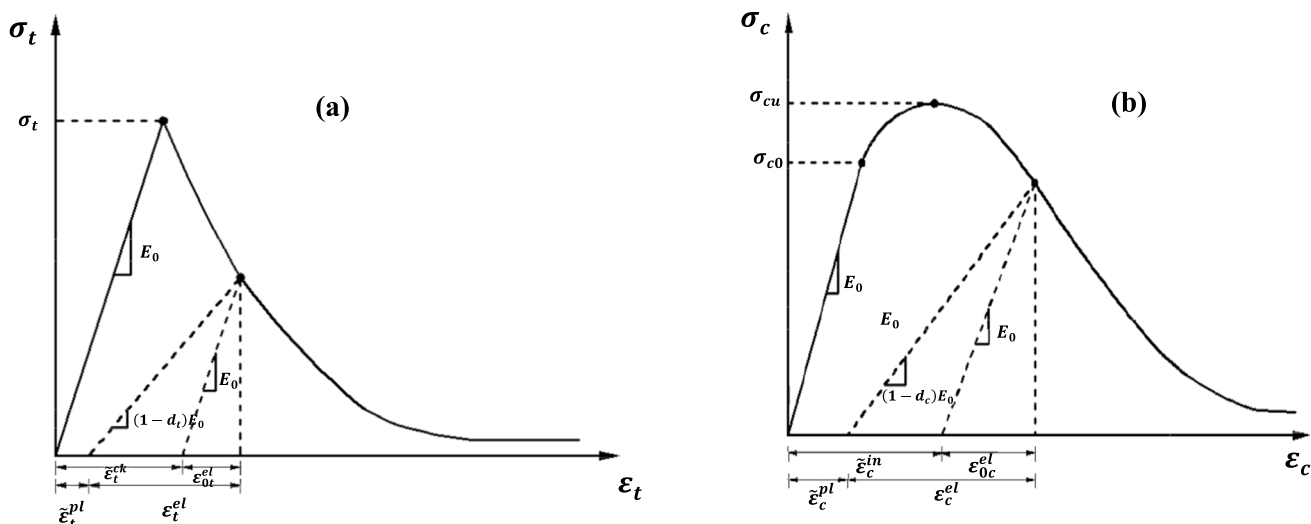


Fig. 6 Response of concrete to uniaxial loading: **a** behavior under tensile stress; **b** behavior under compressive stress (Abaqus 2014)

$$\sigma_c = \sigma_{cu} \left[2 \left(\frac{\epsilon_c}{\epsilon_c'} \right) - \left(\frac{\epsilon_c}{\epsilon_c'} \right)^2 \right] \tag{5}$$

where $\epsilon_c^{in,h}$ is the inelastic compressive strain, E_0 is the initial tangent modulus of elasticity, and ϵ_c is the total compressive strain, σ_{cu} and is ultimate compressive strength.

• **Uniaxial tensile behavior**

The stress–strain relationship under tension Fig. 6a includes a linear branch of elastic strain that represents concrete's pre-failure behavior and a nonlinear branch of plastic strain that illustrates concrete's post-failure behavior (Santos et al. 2020; Jafarian et al. 2020).

The tensile strength σ_{t0} was taken 7% to 10% of maximum compressive strength σ_{cu} , and the maximum value was used in this investigation is $\sigma_{t0} = 0.1 \sigma_{cu}$, 1% of the tensile strength was considered in this research, the correspondence strain value where stress is

1% of the ultimate tensile strength, was taken as 10 times the percentage of the strain (Hafezolghorani et al. 2017).

In addition, the plastic hardening strain in tension ($\epsilon_t^{pl,h}$) is given by (Hafezolghorani et al. 2017) in (Eq. 6):

$$\epsilon_t^{pl,h} = \epsilon_t^{ck,h} - \frac{d_t}{1 - d_t} \frac{\sigma_t}{E_0} \tag{6}$$

where $\epsilon_t^{ck,h}$ is the cracking strain in tension, d_t is the tensile damage parameter, and σ_t is the tensile stress are given in the following equations:

$$d_t = 1 - \frac{\sigma_t}{\sigma_{t0}} \tag{7}$$

$$\epsilon_t^{ck,h} = \epsilon_t - \frac{\sigma_t}{E_0} \tag{8}$$

$$\sigma_t = (1 - d_t) E_0 (\epsilon_t - \epsilon_t^{pl,h}) \tag{9}$$

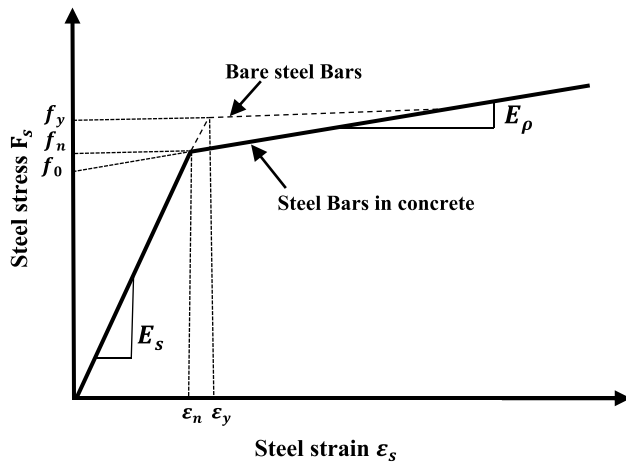
where ϵ_t is the total tensile strain.

3 Additional CDP parameters

In addition to the elastic parameters, such as the elasticity module and Poisson coefficient, the CDP constitutive model also includes other plastic characteristics to fully represent the behavior of concrete. The dilation angle Ψ is the internal friction angle of concrete and has a significant influence on the ductility of the material. Therefore, the ductility value increases in direct proportion to the angle. A small positive parameter that represents the rate of approach of the plastic potential hyperbola to its asymptote is called eccentricity. The parameter σ_b/σ_{b0} is the ratio between the compressive strengths in the biaxial and uniaxial states and it is obtained from 1.1 to 1.16 in tests. K value is the ratio of the tensile to the compressive meridian, its value ranges from 0.5 to 1, and the viscosity parameter shows visco-plastic resting time (Rafati and Razavi 2016; Santos et al. 2020). All the parameters mentioned in the preceding paragraph are shown in Table 2.

Table 2 CDP concrete material parameters

Concrete MPa	Young's Modulus	Poisson's Ratio	Dilation angle	Eccentricity	σ_b/σ_{b0}	K	Viscosity Parameter
43	30,819,96	0,2	35	0,1	1,16	0.667	0,007,985

**Fig. 7** Average stress–strain relationships of steel reinforcement using bilinear model (Belarbi and Hsu 1994)**Table 3** Material properties of steel reinforcement

Diameter (mm)	F _y (MPa)	F _u (MPa)	Elongation (%)	E _s (GPa)
12.7	432	508	14	200
6	496	532	4.67	232

4 Steel Bar Model

The modeling of the reinforcements steel bar was made according to the law of bilinear behavior. The bilinear model of the average stress–strain relationship of reinforcing bars embedded in concrete is illustrated graphically in Fig. 7. Both longitudinal and transverse reinforcements are affected by this relationship (Belarbi and Hsu 1994). Table 3 illustrates the material properties of steel reinforcement used in this study.

5 The CFRP model

The CFRP composites are anisotropic materials that do not have the same properties in all directions. In this study, the linear elastic orthotropic properties of CFRP were assumed. In addition, CFRP is a brittle material that needs to define the hashin damage only (Rafati and Razavi 2016). As shown in Table 4, the tensile strength, elasticity

Table 4 Material properties of CFRP

Material	Design thickness (mm)	Modulus of elasticity (GPa)	Ultimate Elongation (%)	Tensile strength (MPa)
SikaWrap 230 c	0.129	220	1.7	3200

modulus, and ultimate elongation are the material properties used in the numerical study for CFRP wraps.

6 Boundary Conditions and Loading

Hinger and roller supports were used to simulate the reactions of all specimens' supports, while the load was applied at the top of the column. The locations of the supports for the models were characterized by a/d ratio, of 1.0, 0.7, and 0.5. As shown in Fig. 5, all models are loaded based on controlling maximum load of 800 KN.

6.1 Nonlinear Solution

Several static stress analysis procedures are available in Abaqus/Standard. One of which has been employed herein in this FE analysis. The chosen procedure is usually used for stable problems and when inertia effects are neglected. It can incorporate a linear or nonlinear responses. Nonlinear structural analysis was performed in this work utilizing Newton's approach. This nonlinear analysis includes a large displacement effect, material nonlinearity, and geometrical nonlinearity. To solve nonlinear equilibrium equations, Abaqus/Standard uses Newton's method. The problem involves history-dependent response. Therefore, the solution is usually obtained as a series of increments with iterations to obtain equilibrium within each increment (Abaqus 2014).

The step option is used to define the analysis method, period time and increments, and other factors, the program must take into account when running the simulation. A time step has been defined, with the initial time increment assigned to 0.01 and the time period of the step set to 1.0. The minimum time increment has been set to 10⁻⁴, the maximum time increment has been adjusted to 0.1, and the maximum number of increments in a step has been set to 1,000,000 in order to avoid limiting the analysis and imposing its termination. The default automatic incrimination scheme was selected because it will select increment sizes

based on computational efficiency in ABAQUS (Abaqus 2014).

6.2 Identification and Strengthening of Corbel Models

As shown in Fig. 8 and Table 5, nine RC corbels were developed and analyzed. In order to validate the numerical simulation, the results of the finite element models are compared to those of the experimental tests from previous studies. Two corbels were kept as control specimens CONT1 and CONT3 without any external composite reinforcement, with different ratios of a shear span-to-effective depth of 0.7 and 0.5, respectively. Seven additional corbels are analyzed, they are characterized by three different configurations of strengthening: horizontal CFRP strips for corbel specimens CHS2 and CHS4, inclined configuration for corbel

specimens CIS2 and CIS4, and combined configuration for corbel specimens CISR2, for investigating the effect of the shear span-to-depth ratio (a/d) and the influence of direction and amount of CFRP on the behavior of reinforced concrete corbel. The comparisons are shown in the form of load–deflection curves.

7 Validation of the Proposed Numerical Model

7.1 Load–Deflection Response

As shown in Table 6, the numerical model was effectively validated and matched with the previously selected experimental studies (Abed Attiya and Mohamad-ali 2012). The results indicate that the experimental and numerical values

Fig. 8 Corbels CFRP configurations

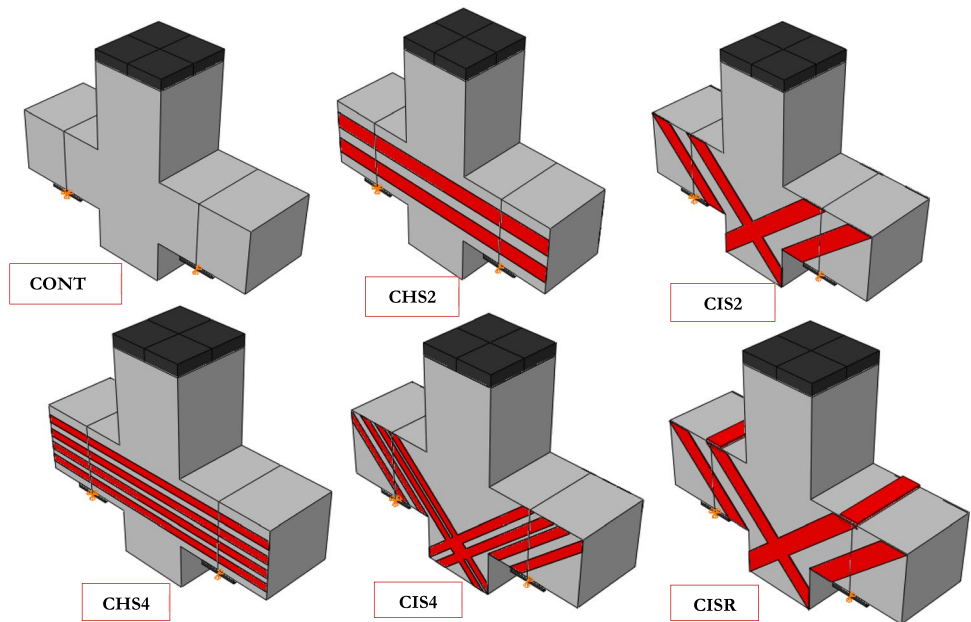


Table 5 Details of the tested corbel (Abed Attiya and Mohamad-ali 2012)

Test reference	Compressive Strength (MPa)	Tensile Strength (MPa)	Ratio (a/d)	CFRP Width (mm)	CFRP orientation	Number of CFRP strips
CONT1	47.57	2.11	0.7	–	–	–
CONT3	45.72	2.50	0.5	–	–	–
CHS2	47.57	2.11	0.7	36	Horizontal	2 CFRP–2 side
CHS4	46.46	2.52	0.7	18	Horizontal	4 CFRP –2 side
CIS2	43.16	2.35	0.7	36	Inclined 45°	2 CFRP –2 side
CIS4	45.28	2.51	0.7	18	Inclined 45°	4 CFRP –2 side
CISR2	46.31	2.62	0.7	36	Inclined 45°	2 CFRP –4 side
CISR2	42.90	2.70	1.0	36	Inclined 45°	2 CFRP –4 side
CISR2	46.31	2.59	0.5	36	Inclined 45°	2 CFRP –4 side

Table 6 Finite element and experimental results of the corbel specimens

Corbel label	a/d ratio	Ultimate Load (KN)		Deflection (mm)		P_{num}/P_{exp}	Increase of Ultimate Load %
		Exp	Num	Exp	Num		
CONT1	0.7	292	301	3.29	3.22	1.031	–
CONT3	0.5	358	350.1	1.94	2.01	0.977	–
CHS2	0.7	335	333.11	2.75	2.45	0.994	11
CHS4	0.7	347	351	3.58	3.48	1.011	17
CIS2	0.7	430	432.92	3.45	4.1	1.006	44
CIS4	0.7	425	428.16	2.97	4.02	1.007	42
CISR2	0.7	467	472.93	3.73	3.9	1.012	57
CISR2	0.5	504	500.1	3.05	2.87	0.992	66
CISR2	1.0	294	300	3.43	3.59	1.021	–

of the ultimate load capacity and the corresponding deflection were quite equal. The results are also similar to those obtained by (Sayhood et al. 2016; Ivanova et al. 2020) in terms of the evolution of ultimate load capacity and deflection at ultimate load, despite the fact that the factors studied are not the same.

Figures 9,10,11,12 represent the results of the load–deflection responses of the RC corbels with and without strengthening that are plotted from the numerical model and experimental testing. The results indicate a good correlation. It seems that the load–deflection curves are pretty much identical, which is more clear through Fig. 13a, b showing the comparison between the maximum experimental and numerical ultimate load and the deflection at the mid-span. The analysis proved that there is no statistically significant difference between the results of the experiment

and numerical results, and it can be concluded that there is a great consistency in term of maximum load and deflection.

As can be seen from Figs. 9 and 12, the reduction in the shear span-to-effective depth a/d leads to an increase in the ultimate load of the corbel and a decrease in the deflection value. Unstrengthened specimens CONT1 and CONT3 with $a/d=0.7$ and $a/d=0.5$, respectively, exhibited load capacities of 301 kN and 350.1 kN, respectively, which means a gain of strength by 16%. However, the strengthened corbel specimens CISR2 with three different values of shear span-to-effective depth equal to 1.0, 0.7, and 0.5 exhibited load capacities of 300 kN, 472 kN, and 500 kN, respectively, which means a gain of strength by 66%.

In order to investigate the effect of strengthening by externally bonded CFRP strips, CHS2 and CHS4 were strengthened with one layer of horizontal CFRP strips, and CIS2 and

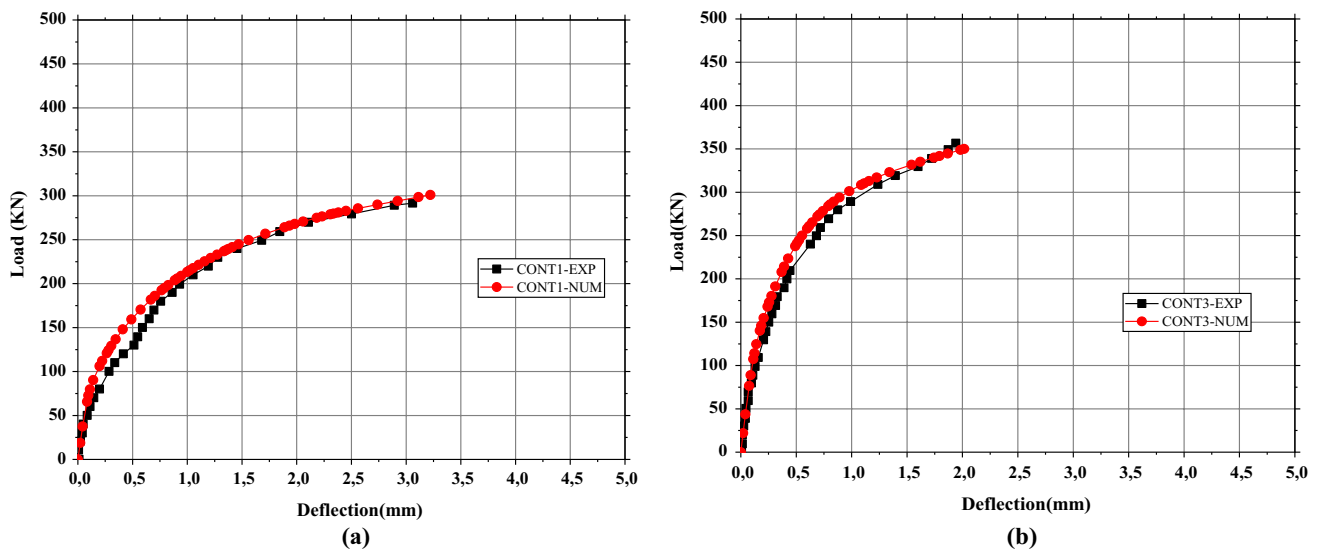


Fig. 9 Comparison between experimental (Abed Attiya and Mohamad-ali 2012) and numerical curves of control corbel specimens: **a** corbel CONT1; **b** corbel CONT3

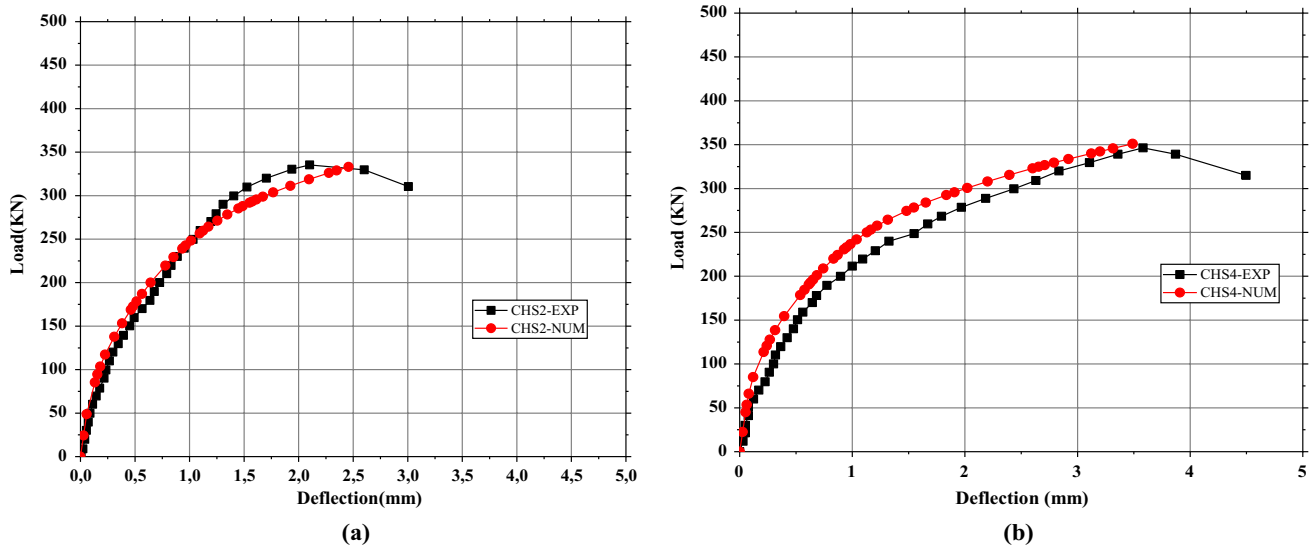


Fig. 10 Comparison between experimental (Abed Attiya and Mohamad-ali 2012) and numerical curves of CHS corbel specimens: **a** Corbel CHS2, **b** Corbel CHS4

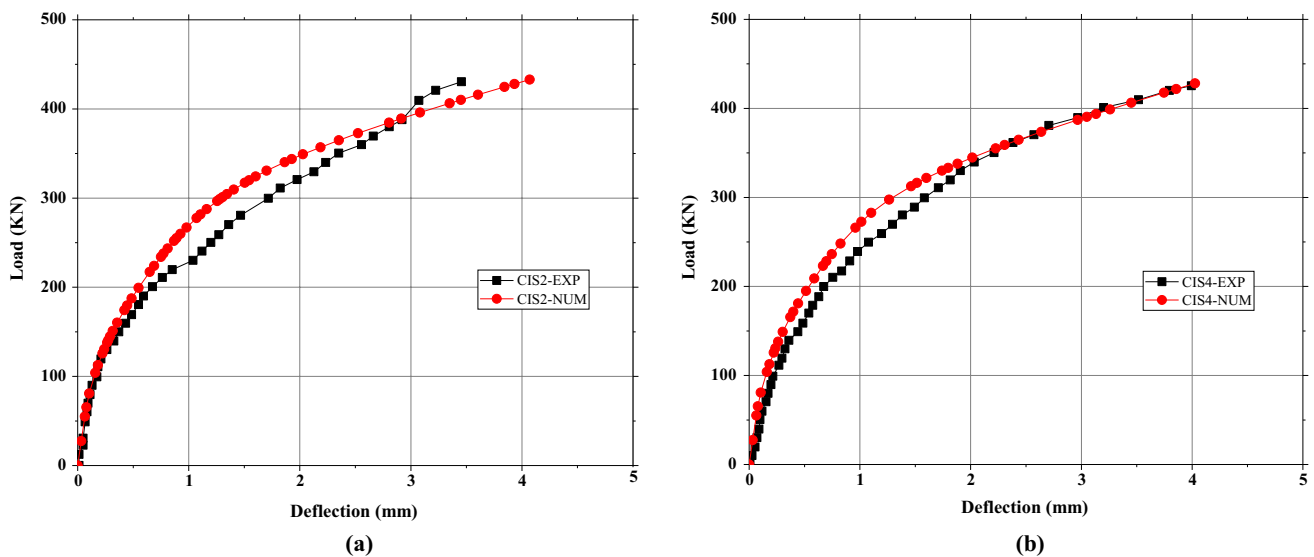


Fig. 11 Comparison between experimental (Abed Attiya and Mohamad-ali 2012) and numerical curves of CIS corbel specimens **a** Corbel CIS2, **b** Corbel CIS4

CIS4 were strengthened with one layer of inclined CFRP strips. Hence, CISR2 was strengthened with one layer of horizontal and inclined CFRP strips. As can be observed from Fig. 14, which describes the effect of strengthening on the load–deflection, the corbels strengthened with a horizontal shape significantly improved the ultimate load by 17%, and the corbel specimens strengthened with an inclined shape improved the ultimate load by 44%. While corbels strengthened with a horizontal and inclined reached 57% improvement in load-carrying capacity. This growth is mainly attributed to the arrangement of the CFRP strips

being perpendicular to the inclined fractures, which covered the corbel's shear-critical zone as shown in previous studies (Abed Attiya and Mohamad-ali 2012; Sayhood et al. 2016).

It can be concluded that the external CFRP reinforcement has a significant impact on the load capacity of the corbels. The shear span-to-effective depth ratio a/d and the amount and direction of the CFRP strips are all important criteria impacting the load-carrying capacity of the RC corbel.

To further demonstrate the reliability of the numerical model, two corbel specimens that were experimentally tested earlier by (Al-Kamaki et al. 2018) were numerically

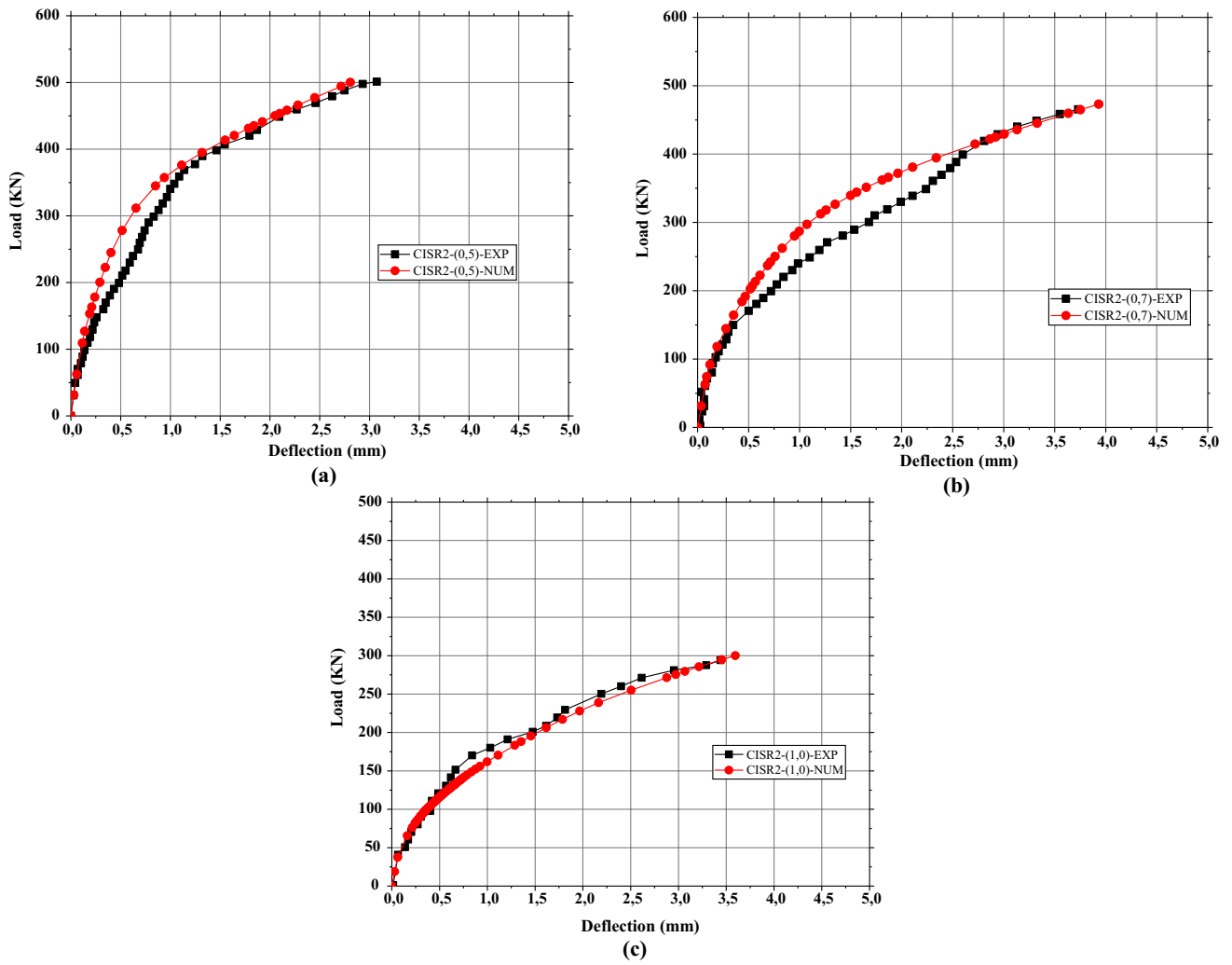


Fig. 12 Comparison between experimental (Abed Attiya and Mohamad-ali 2012) and numerical load–deflection curves of corbel CISR specimens **a** Corbel CISR2 with $a/d=0.5$ **b** Corbel CISR2 with $a/d=0.7$ **c** Corbel CISR2 with $a/d=1.0$

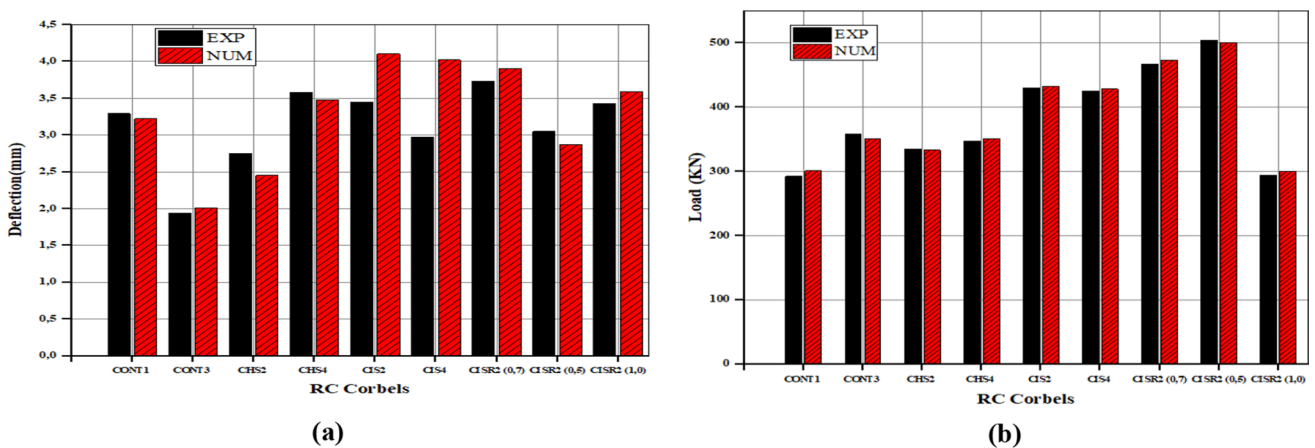


Fig. 13 Comparison between ultimate experimental and numerical values: **a** ultimate deflection; **b** ultimate load

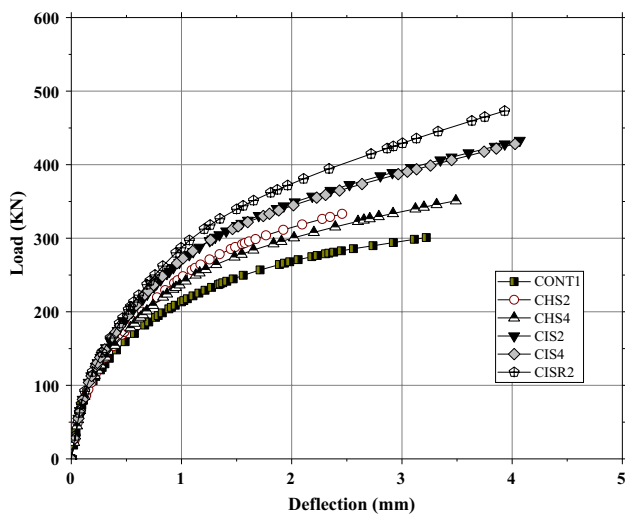


Fig. 14 Load–deflection curves of corbel specimens with different shapes of CFRP

validated, and designated CN WO and HOR WO, respectively. CN WO served as a control corbel without horizontal stirrups, while HOR WO was strengthened with a single layer of CFRP and similarly lacked stirrups. The numerical results are shown in Fig. 15.

The load–deflection curves for the corbel specimens CN WO and HOR WO, from both numerical and experimental testing by (Al-Kamaki et al. 2018), are shown in Fig. 15a, b. The accuracy of the numerical model was demonstrated by the close correlation between the load–deflection curves of the two corbels at various response stages. Particularly, at the linear region where the curves are stiffer and closer. The

numerical results have good agreement with the experimental results with only a small deviation of 0.98 for the ultimate load and ultimate deflection for both corbel specimens CN WO and HOR WO. This indicates that the present numerical model is accurate.

7.2 Deflection Evolution

Numerical measurements of deflection values under varying loading conditions have been taken from three separate corbel specimens in order to demonstrate the effect of the CFRP strips on corbel strength. The studied corbel specimens are CONT1 with no strengthening, CHS2 strengthened with horizontal CFRP strips, CIS2 strengthened with inclined CFRP. The measurement was in three different points: at the right and left near the bearing plate, and at the mid-span of the corbel. As shown in Fig. 16 which describes the deflection shapes of corbel specimens CHS2, and CIS2, compared to the unstrengthened corbel specimen CONT1. It can be seen that the two strengthened corbels CHS2 and CIS2 have a high degree of strength. Moreover, Fig. 17 represents the relationships between loads and deflections, as can be observed the load and deflection have a relative relationship. The deflection is generally increasing with further loading at any point of each corbel.

The results of the deflection evolution at particular load stages in Fig.17a, b, c showed that the highest deflection values recorded are at point 2. The measurements were 3.22 mm, 2.45 mm, and 4.1 mm during applying loads equal to 300 kN, 333 kN, 433 kN for corbel specimens CONT1, CHS2, and CIS2, respectively. Hence, the lowest deflection values are at the point 1, with measurements of 0.0078 mm,

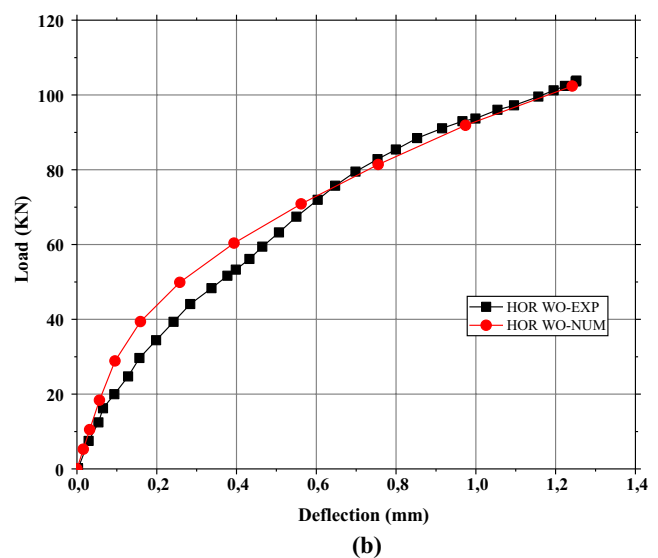
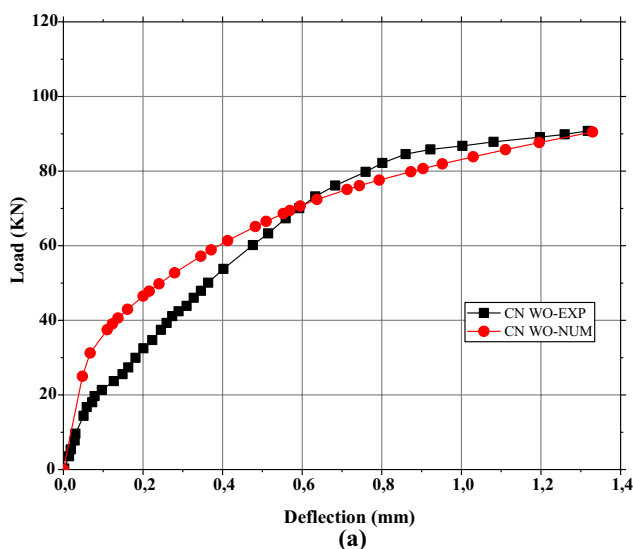


Fig. 15 Comparison between experimental (Al-Kamaki et al. 2018) and numerical load–deflection curves of corbel: **a** CN-WO; **b** HOR-WO

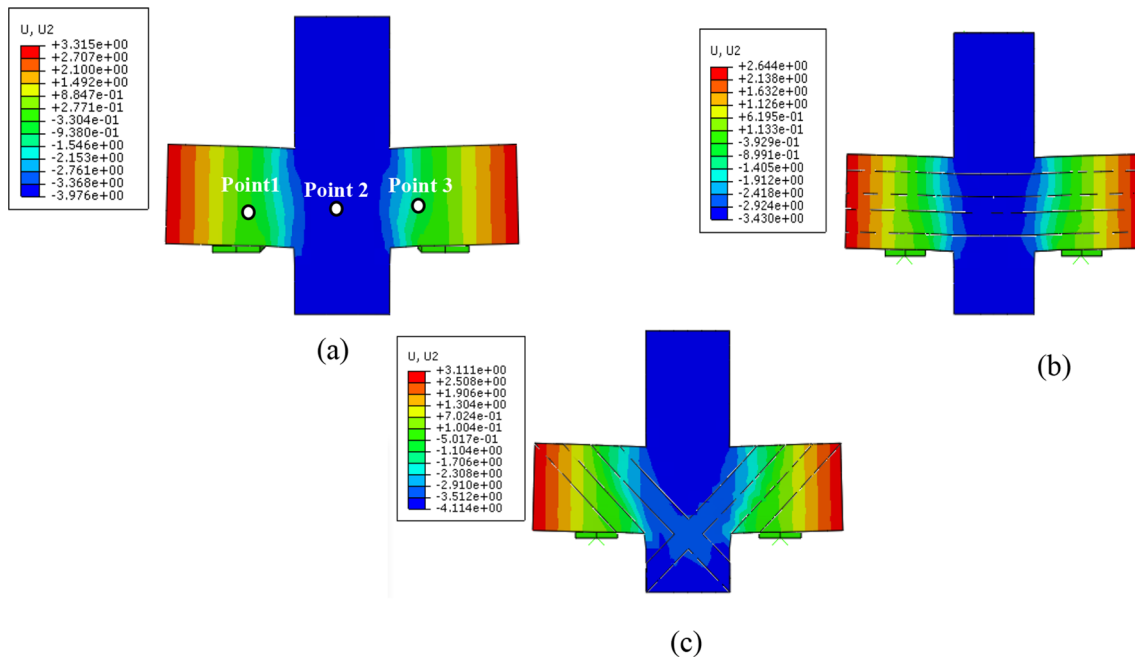


Fig. 16 Model deflections throughout RC corbels (mm): **a** CONT1; **b** CHS2; **c** CIS2

0.0081 mm, and 0.01 mm, when applying loads equal to 20 kN, 21 kN, 27 kN for corbel specimens CONT1, CHS2, and CIS2, respectively. The stiffness and strength of the corbels are varying, the strengthened corbels CHS2 and CIS2 exhibited higher stiffness compared to unstrengthened corbel specimen CONT1. This result confirms that the external composite reinforcement CFRP enhanced the strength of the corbels. Moreover, considering the direction and the amount of CFRP strips, the corbel strengthened with inclined CFRP strips showed greater stiffness and more ductile behavior than the specimens with horizontal CFRP strips as shown in Fig. 16b, c. In addition, there is an increase in the shear capacity of the corbel by 44% for CIS2, this value is due to the effectiveness of CFRP strips in preventing the growth and spread of created shear cracks.

8 Parametric Analysis

The majority of the existing research in the literature on strengthening RC corbels has concentrated on either experimentally or analytically investigating their structural behavior, or both, with the goal of identifying the most important parameters influencing corbel performance. To evaluate the effects of such parameters on the strength of RC corbel, a comprehensive parametric numerical study was conducted on four corbel specimens (designed

CONT1, CHS2, CIS2, and CISR2) by varying critical factors such as the thickness of CFRP strips, the compressive strength of concrete, and the inclusion of secondary reinforcement.

Several indicators were chosen in order to estimate the enhancement of the reinforcement performances. In addition to the ultimate load and deflection at ultimate load, the ductility, the stiffness, and the flexural toughness are selected. The ultimate load and deflection at ultimate load indicate the improvement in shear capacity. The ductility is a pointer recounting reinforced concrete members' adequacy to sustain essential plastic deformations without a vital reduction in their peak strength. The ductility index represents the total area ratio under the load–deflection curve to a partial area extended up to the service loads, which were supposed 75% of their peak loads according to recommendations of prior studies (Mahalhal et al. 2021; Spadea et al. 1997). The stiffness can be assessed using the secant stiffness which represents the slope of a line linking the origin point of the load–deflection response with the point of ultimate loads. In the case of the flexural toughness, it defines the efficiency of concrete members to absorb energy without displaying a substantial reduction in their strength. This mensuration is equivalent to the total area under the load–deflection response (Mahalhal et al. 2021). The calculated values of these indicators are addressed in Table 7, Table 8, and Table 9 depending on the critical studied factor.

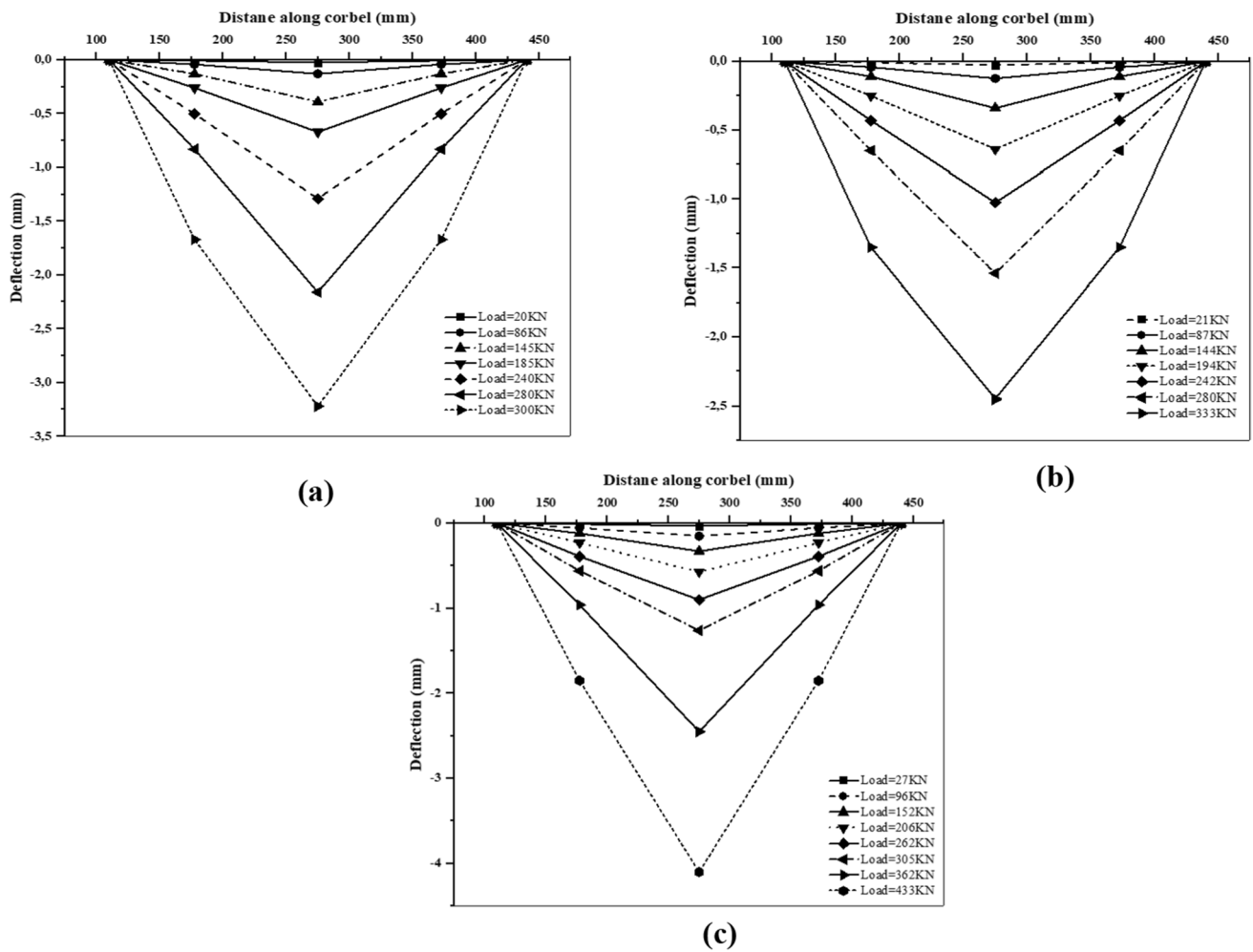


Fig. 17 Reinforced concrete corbels deflection at particular load stages: a CONT1; b CHS2; c CIS2

Table 7 Test results of corbel specimens with different number of layers of CFRP

Corbel label	Number of layers	Ultimate Load (kN)	Increase of Ultimate Load %	Deflection at Ultimate Load (mm)	Ductility index	Secant stiffness (kN/mm)	Flexural toughness (kN.mm)
CONT1	No layers	301	-	3.22	3,73	93,48	969,22
CHS2	01 layer	333	11	2.45	3,20	135,92	815,85
	02 layers	400	33	3.34	3,37	119,76	1336
	03 layers	500	66	4.28	3,14	116,82	2140
CIS2	01 layer	433	43	4.1	3,42	105,61	1775,3
	02 layers	501	66	4.01	3,15	124,94	2009,01
	03 layers	567	88	4.6	3,04	123,26	2608,2
CISR2	01 layer	472	56	3.9	3,06	121,03	1840,8
	02 layers	588	95	4.09	2,84	143,77	2404,92
	03 layers	672	123	4.51	2,82	149,00	3030,72

Table 8 Test results of corbel specimens with different compressive strength of concrete

Corbel label	f'_c (MPa)	Ultimate Load(kN)	Increase of Ultimate Load %	Deflection at Ultimate Load (mm)	Ductility index	Secant stiffness (kN/mm)	Flexural toughness (kN.mm)
CONT1	30	212	–	3.38	3,34	62,72	716,56
	47	301	42	3.22	3,73	93,48	969,22
	50	350	65	3.13	3,07	111,82	1095,50
CHS2	30	254	–	2.91	3,50	87,29	739,14
	47	333.11	31	2.45	3,20	135,96	816,12
	50	400	57	2.67	2,97	149,81	1068,00
CIS2	30	326	–	3.44	3,19	94,77	1121,44
	43	432.92	33	4.1	3,42	105,59	1774,97
	50	450	38	3.33	3,29	135,14	1498,50
CISR2	30	393	-	3.81	2,94	103,15	1497,33
	46	472.93	20	3.9	3,06	121,26	1844,43
	50	500	27	3.29	2,74	151,98	1645,00

Table 9 Test results of corbel specimens with and without stirrups

Corbel label	Ultimate Load (kN)	Increase of Ultimate Load %	Deflection at Ultimate Load (mm)	Ductility index	Secant stiffness (kN/mm)	Flexural toughness (kN.mm)
CONT1	301	–	3.22	3,73	93,48	969,22
CONT1 + 2S	350	16	3.53	4,17	99,15	1235,5
CHS2	333	–	2.45	3,20	135,92	815,85
CHS2 + 2S	375	13	2.87	3,64	130,66	1076,25
CIS2	433	–	4.1	3,42	105,61	1775,3
CIS2 + 2S	500	15	3.57	3,40	140,06	1785
CISR2	472.93	–	3.9	3,06	121,26	1844,427
CISR2 + 2S	500	6	3.35	3,31	149,25	1675

8.1 Effect of the Number of CFRP Layers

As a case study, the impact of the thickness of CFRP strips on the behavior of RC corbels reinforced with CFRP was investigated using three corbel specimens, CHS2, CIS2, and CISR2. These specimens were strengthened with three different values of CFRP layers (one layer, two layers, and three layers), whereas the control corbel specimen CONT1 was left unreinforced and used as a reference. The results are reported in Table 7 and Fig. 18. As seen, the shear capacity and toughness of the corbels improve as the thickness of the CFRP strips rises. However, the ductility doesn't follow the same trend. The studied reinforcement configurations showed a progressive reduction in ductility of RC corbels. This is in conformity with several previous studies (El-Refaie et al. 2003; Maghsoudi and Bengar 2011; Al-Rousan et al. 2012; Njeman et al. 2018). According to Maghsoudi and Bengar (2011), the decrease of the ductility is usually linked to premature failures, such as intermediate Crack, debonding of FRP, plate end interfacial debonding, and

cover separation. Regarding to the stiffness, all reinforcement configurations show higher stiffness. Especially, the strengthened RC corbels with three layers of CFRP, they are stiffer than the corbel specimens with one or two layers of CFRP, showing that the improvement's level varies with the thickness.

The ultimate load and deflection data of strengthened specimens with one layer of CFRP strips (Table 7) show an increase in the shear capacity of the corbel specimen of 11%, 43%, and 56% for CHS2, CIS2, and CISR2, respectively, compared to the unstrengthened corbel specimen CONT1. For corbel specimens CHS2, CIS2, and CISR2 that were reinforced with three layers of CFRP strips, the maximum ultimate loads were 500 kN, 567 kN, and 672 kN, respectively. This is attributable to an increase in the corbel's ultimate shear strength (Ivanova et al. 2015).

In the case of specimens strengthened with inclined CFRP strips, the shear capacity and deflection values of all RC corbel specimens showed a greater degree of improvement. This is remarkable in configuration CIS2 and particularly in

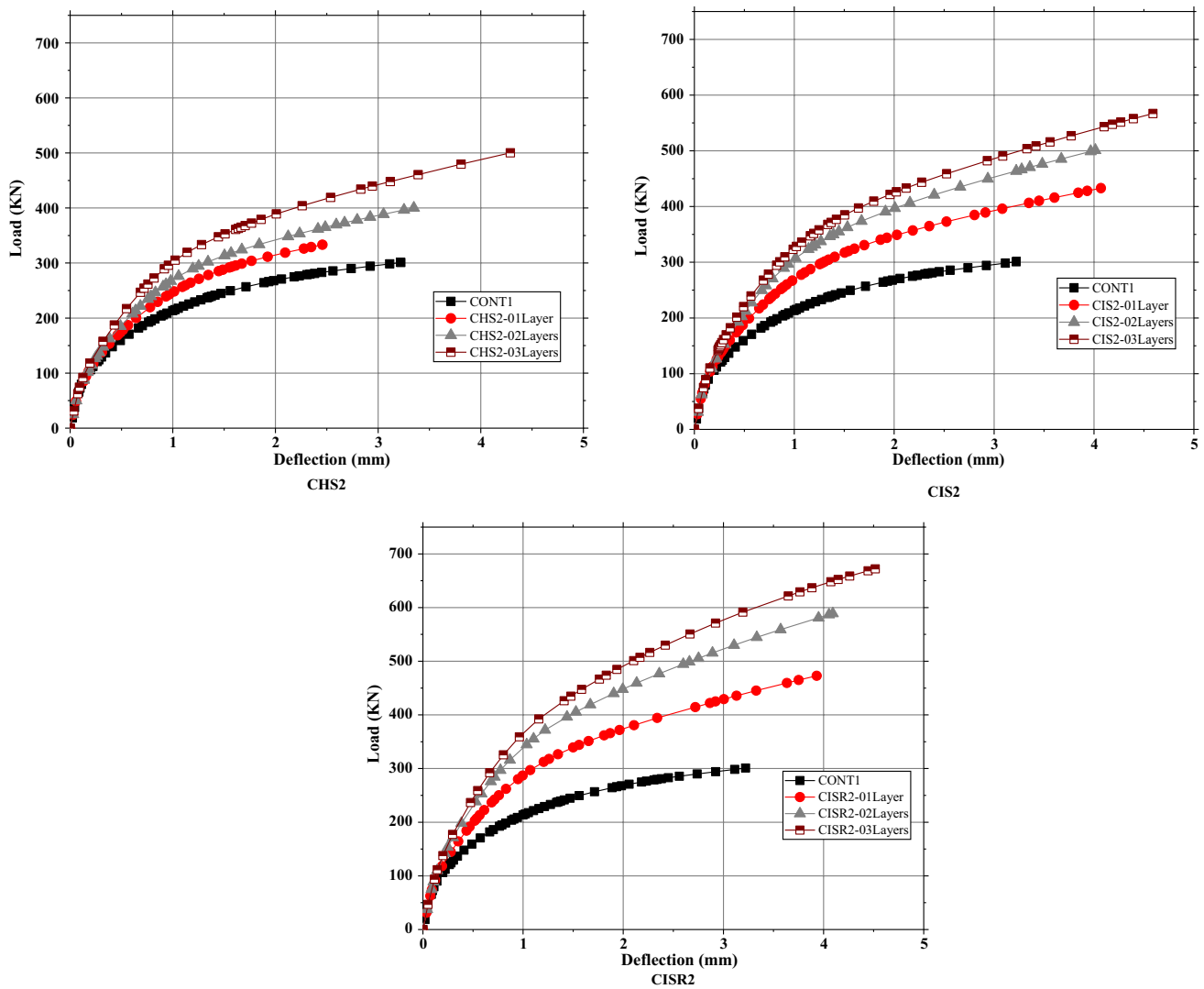


Fig. 18 Load–deflection curves of corbel specimens with different number of layers of CFRP

CISR, compared to specimens strengthened with horizontal CFRP strips (case of configuration CHS2).

The improvement for CIS2 and CISR2 was 88% and 123%, respectively, as illustrated in Fig. 18. This is because the CFRP strips' inclined composite reinforcement covers the corbel's shear-critical zone, preventing the propagation and development of produced shear cracks (Sayhood et al. 2016).

8.2 Effect of Compressive Strength of Concrete f'_c

The impact of concrete compressive strength on the behavior of RC corbels reinforced with CFRP strips was examined using the suggested numerical model. Three distinct concrete compressive strengths 30 MPa, 47 MPa, and 50 MPa were tested using corbel specimens CONT1, CHS2, CIS2, and CISR2. All other corbel specimen

evaluation parameters remained the same. The influence of (f'_c) on the performance of corbel specimens is seen in Fig. 19. According to the load–deflection curves, the compressive strength of concrete (f'_c) is a crucial factor influencing the behavior of RC corbels. The maximum load of the CONT1 corbel increases from 212 kN at $f'_c = 30$ MPa to 350 kN at $f'_c = 50$ MPa, with a 65% improvement over the unreinforced corbel.

In addition, the ultimate load of all modeled corbels, stiffness and flexural toughness increase when rising the compressive strength (Table 8). The results of ductility remain variable depending of reinforcement configuration. As indicated in earlier research (Abdulridha et al. 2018), increasing the compressive strength of reinforced corbels CHS2, CIS2, and CISR2 from 30 to 50 MPa led to an increase in shear capacity of 57%, 38%, and 27%, respectively, as well as a decrease in deflection values, as shown in Table 8's results.

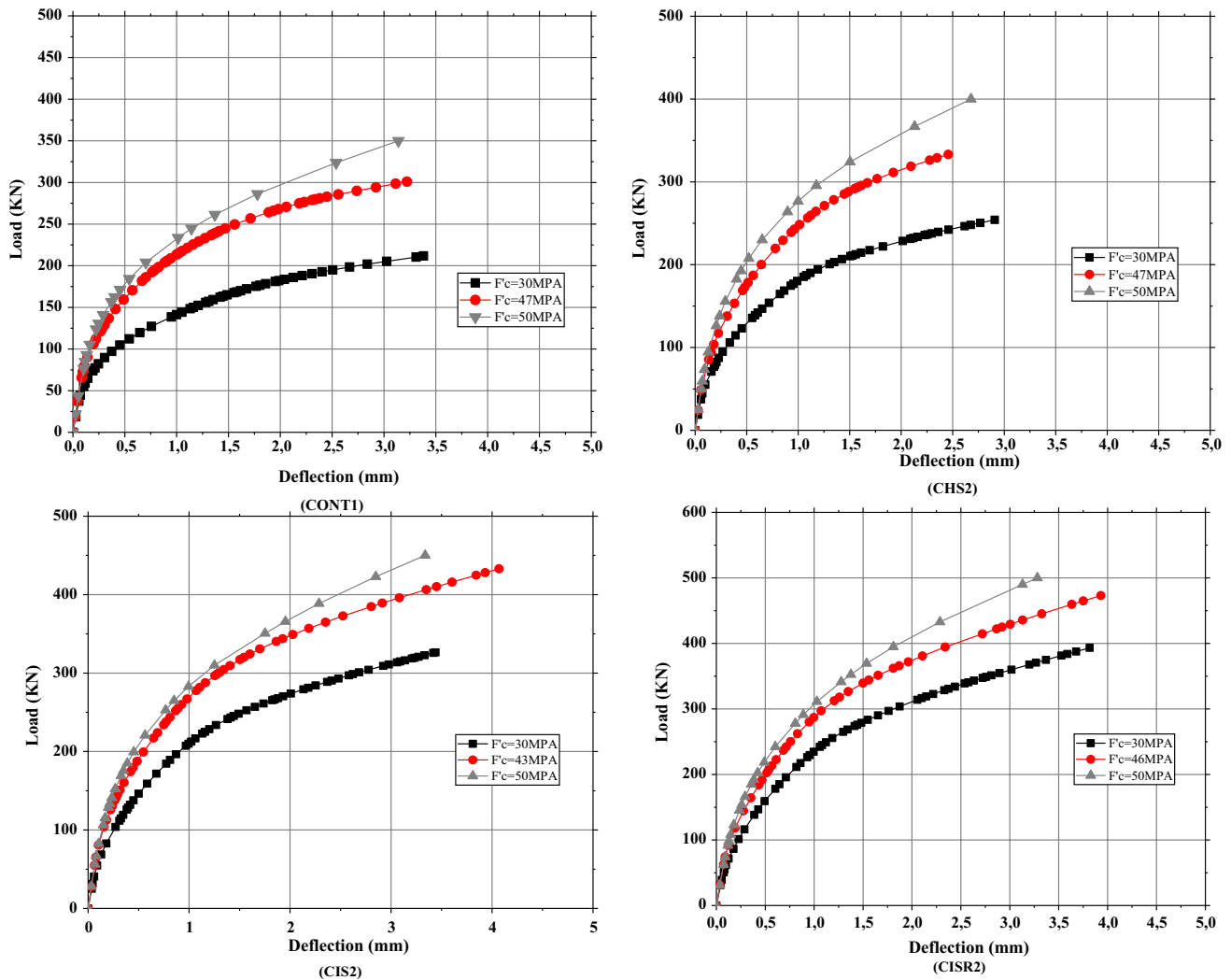


Fig. 19 Load–deflection curves of corbel specimens with different compressive strength of concrete

From the mentioned results, it appears that the compressive strength is the most significant component of concrete that affects corbel behavior since concrete is a very compressive material.

8.3 Effect of the Horizontal Shear Reinforcement (Stirrups)

Corbel specimens CONT1, CHS2, CIS2, and CISR2 were studied without horizontal reinforcement. While corbel models CONT1 + 2S, CHS2 + 2S, CIS2 + 2S, and CISR2 + 2S were analyzed with the addition of two stirrups of six diameter to assess the effect of stirrup presence on RC corbel behavior. The ultimate load, the associated deflection, and the several chosen performance indicators for each model are tabulated in Table 9. The curves for load versus deflection are shown in Fig. 20.

The ultimate loads were 350 kN, 375 kN, 500kN, and 500 kN for corbel specimens CONT1 + 2S, CHS2 + 2S, CIS2 + 2S, and CISR2 + 2S, respectively. These results indicate that when horizontal reinforcement stirrups are added, the shear capacity improves by 16%, 13%, 15%, and 6%, respectively, in comparison with corbel specimens lacking horizontal steel reinforcement. The inclusion of horizontal reinforcement stirrups clearly boosts ductility, stiffness and flexural toughness. This is in conformity with previous studies (Maghsoudi and Bengar 2011). In addition, the presence of steel stirrups has a positive effect on the strength of RC corbels, offering a slight improvement in corbel strength and decreasing corbel deflection. Specimens without stirrups showed all a higher deflection than specimens with stirrups. Moreover, when horizontal reinforcement stirrups are present, an increase in shear capacity, in ranges between 6 and 16% was observed, as indicated in previous studies (Al-Kamaki et al. 2018).

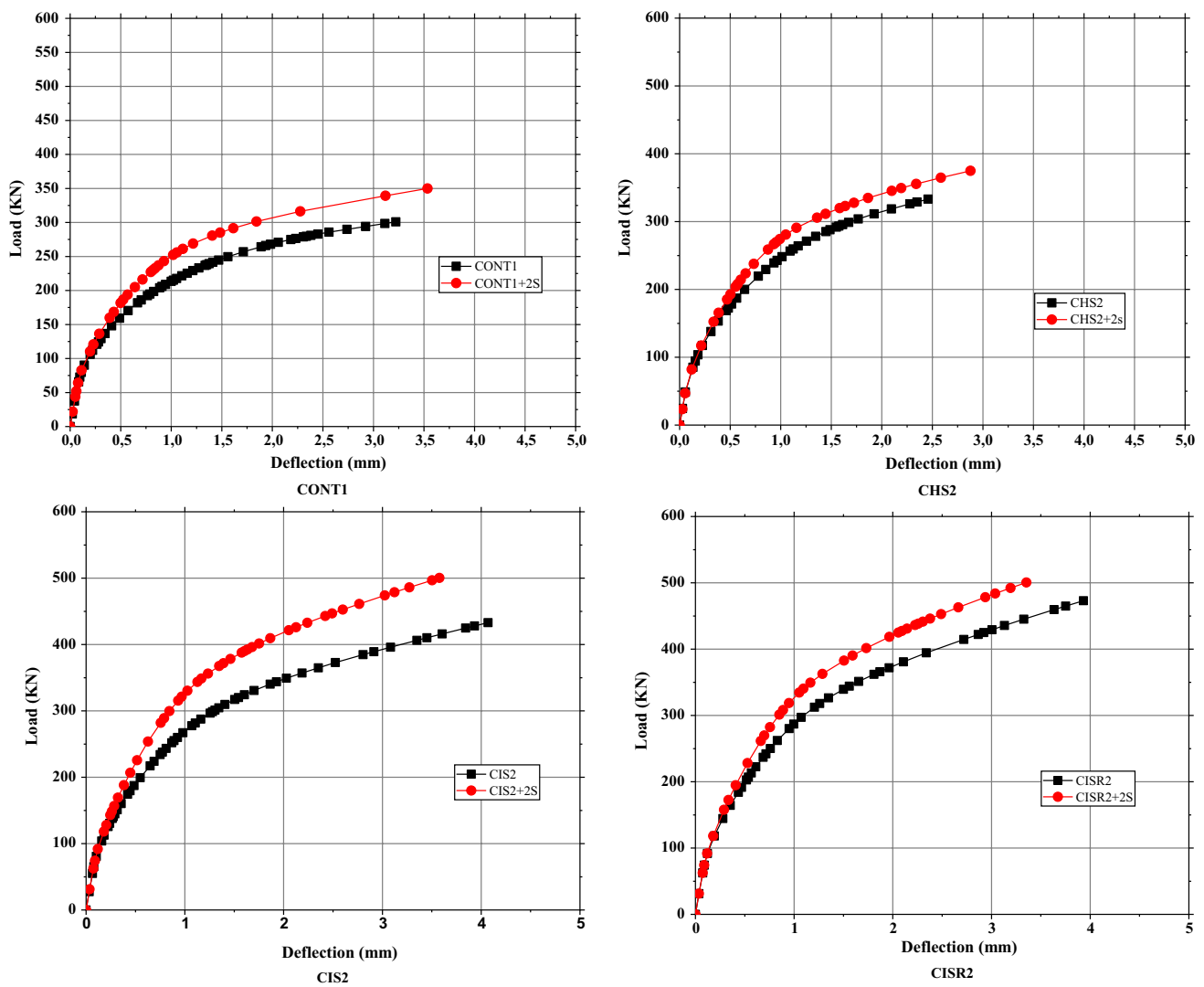


Fig. 20 Load–deflection curves of corbel specimens with and without stirrups

Additionally, the secondary reinforcements provide a significant role in improving the corbels' crack distribution. This situation leads confining the concrete area producing the diagonal strut, reducing fracture widths, increasing the stiffness and ductility of the corbel, and preventing sudden collapses (Canha et al. 2014).

8.4 The Pattern Cracks and Failure Mode

It should be mentioned that the chosen study did not display the experimental failure mechanisms and crack patterns of all the validated corbels, not allowing the comparison with the numerical ones. As a direct result of this, only numerical predictions of the failure modes have been carried out.

- Control specimen (CONT1)

The crack progression of the control corbel CONT1 is shown in Fig. 21. Figure 21a shows clearly that the initial vertical flexural cracks occurred at or close to the point where the column's adjacent face and the corbel's horizontal face intersected. The diagonal shear cracks occurred on both sides of the corbel along the diagonal region between the loading plate and the internal top corner of the corbel as illustrated in Fig. 21b. As flexural cracks progressed with further loading within the column and toward the upper corbel-column junction, these cracks continued to grow and extend. The concrete is crushing in the struts due to a lack of secondary horizontal stirrups, and the failure mode of CONT 1 occurred as a result of the diagonal concrete strut being crushed immediately after the yielding of tension reinforcement, resulting in brittle collapse. In addition, as can be observed in Fig. 21c, the embedding zone between the column and the corbel experiences the

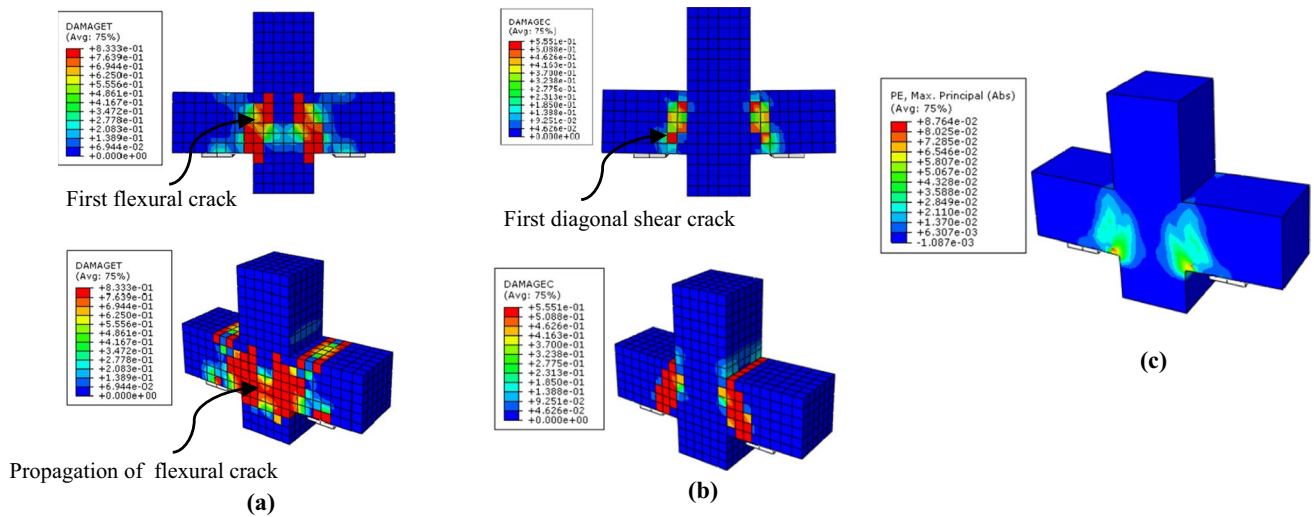


Fig. 21 Corbel CONT1: **a** damage in tension; **b** damage in compression; **c** cracking pattern at ultimate load

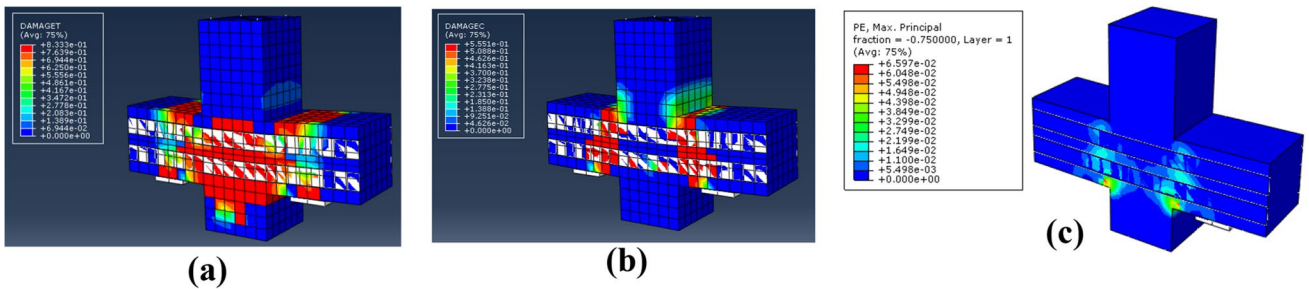


Fig. 22 Corbel CHS2: **a** damage in tension; **b** damage in compression; **c** cracking pattern at ultimate load

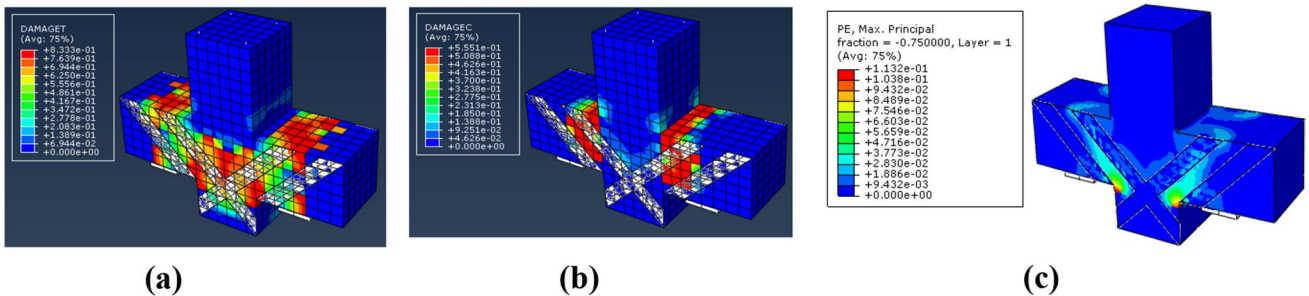


Fig. 23 Corbel CIS2: **a** damage in tension; **b** damage in compression; **c** cracking pattern at ultimate load

highest and most significant stresses, particularly at the bearing plate.

- Strengthened corbel specimens (CHS2, CIS2, CISR2)

Figures 22c, 23c, and 24c illustrate the failure crack patterns of the strengthened corbel specimens CHS2, CIS2, and CISR2. It was observed that all three specimens exhibited the same crack pattern.

Flexural cracks developed vertically at the column-corbels junction as the corbels were loaded as shown in Figs. 22a, 23a, and 24a. Further diagonal shear cracks appeared and developed in the shear span zone as the stress increased. Despite the continuation of the loading, the cracks stopped spreading and expanding as soon as attained as the cracks reached the CFRP strips. The cracks then returned to the inclined path toward the upper corbel-column connection.

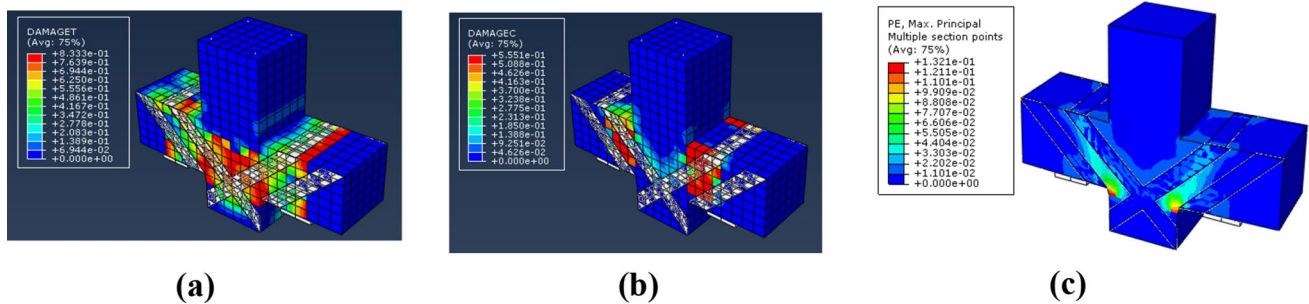


Fig. 24 Corbel CISR2: **a** damage in tension; **b** damage in compression; **c** cracking pattern at ultimate load

Further inclined cracks were caused by increased loading, and the cracks quickly spread until failure, so the mode of failure was by flexure shear and crushing of the diagonal concrete strut.

It should be emphasized that the flexural crack that formed at the intersection of the tension face of the corbel and the face of the column was prevented from expanding and spreading by the external horizontal CFRP composite reinforcement, as illustrated in specimens CHS2 (Fig. 22b). Additionally, the inclined CFRP strips prevented the inclined shear cracks from expanding. The Specimens CIS2 and CISR2 showed this more clearly as illustrated in Figs. 23b, and 24b. It was noticed also from the results that strengthening corbels increased their load capacities and shear strengths by approximately 11%, 44%, and 57% for CHS2, CIS2, and CISR2, respectively.

9 Conclusion

This paper aimed to investigate the behavior of RC corbels strengthened with CFRP strips. Different numerical models were developed and tested by varying in shear span-to-depth ratio with several CFRP configurations. Several conclusions can be drawn according to results of the numerical study:

- The external CFRP composite reinforcement's contribution to load capacity was reduced with increasing shear span-to-effective depth ratio a/d .
- The use of CFRP strips in reinforced concrete corbels provides the ability to enhance shear capacity, stiffness and flexural toughness. In the case of the shear capacity of the corbels increases as the number of layers of CFRP strips rises from one to three layers, with a strong improvement up to 66% for horizontal direction, up to 88% for inclined direction, and up to 123% for combined orientation. Moreover, the ductility index results showed a progressive reduction in ductility of RC corbels for all studied reinforcement configurations.

- The compressive strength of concrete (f_c') has a significant impact on the behavior of reinforced RC corbels. When f_c' was increased from 30 to 50 MPa, the level of load enhancement of corbels attained up to 57%. The numerical results indicate that the inclusion of a secondary reinforcement such as horizontal stirrups provides an extra increase in shear capacity by 16%. It yields to minimize crack widths, improve the ductility, the stiffness, flexural toughness, and results in a less abrupt collapse.
- In terms of failure mechanism, the reinforced RC corbels have more strength, which lead to reducing cracks formation. Therefore, the flexural crack that occurred at the interface of the tension face of the corbel and the face of the column was prevented from developing and expanding.
- The use of inclined CFRP composite for reinforcement can contribute to preventing the expansion and development of diagonal shear cracks.

Declarations

Conflict of interest On behalf of all authors, the corresponding author states that there is no conflict of interest.

References

- Abaqus (2014) Abaqus analysis user's guide. Dassault systèmes, France
- Abdulhaleem KN, Gülşan ME, Çevik A (2018) Mechanical behavior of steel fiber-reinforced self-compacting concrete corbels after exposure to elevated temperatures. *Struct Concr* 19:1881–1894. <https://doi.org/10.1002/SUCO.201700034>
- Abdulridha AJ, Risan HK, Taki ZNM (2018) Numerical analysis of reinforced concrete corbel strengthening by CFRP under monotonic loading. *Int J Civ Eng Technol* 9:1554–1565
- Abed Attiya M, Mohamad-ali AA (2012) Experimental behaviour of reinforced concrete corbels strengthened with carbon fibre reinforced polymer strips. *Basrah J Eng Sci* 12:31–45
- Abu-Obaida A, El-Maaddawy T, El-Ariss B (2020) Numerical simulation of double-sided concrete corbels internally-reinforced with GFRP bars. *Compos Part C Open Access* 2:100040. <https://doi.org/10.1016/J.JCOMC.2020.100040>

- ACI 318 (2019) ACI CODE-318-19: Building Code Requirements for Structural Concrete and Commentary. In: American Concrete Institute, pp 227–232
- Al-Kamaki YSS, Hassan GB, Alsofi G (2018) Experimental study of the behaviour of RC corbels strengthened with CFRP sheets. *Case Stud Constr Mater* 9:e00181. <https://doi.org/10.1016/J.CSCM.2018.E00181>
- Al-Rousan R, Issa M, Shabila H (2012) Performance of reinforced concrete slabs strengthened with different types and configurations of CFRP. *Compos B Eng* 43(2):510–521
- Araújo DL, Azevedo SA, Muniz ED et al (2017) Strength evaluation of concrete corbels cast in a different stage from the column. *Rev IBRACON Estruturas e Mater* 10:509–546. <https://doi.org/10.1590/S1983-41952017000200011>
- Barour S, Zergua A, Bouziadi F, Kaloop MR, El-Demerdash WE (2022) Nonlinear numerical and analytical assessment of the shear strength of RC and SFRC beams externally strengthened with CFRP sheets. *Adv Civ Eng* 2022:1–17. <https://doi.org/10.1155/2022/8741158>
- Belarbi A, Hsu TTC (1994) Constitutive laws of concrete in tension and reinforcing bars stiffened by concrete. *ACI Struct J*. <https://doi.org/10.14359/4154>
- Campione G (2009) Flexural response of FRC corbels. *Cem Concr Compos* 31:204–210. <https://doi.org/10.1016/J.CEMCO.NCOMP.2009.01.006>
- Campione G, Cannella F (2020) Analytical model for flexural response of reinforced concrete corbels externally strengthened with fiber-reinforced polymer. *Aci Struct J* 117:91–102
- Campione G, La Mendola L, Papia M (2005) Flexural behaviour of concrete corbels containing steel fibers or wrapped with FRP sheets. *Mater Struct* 38:617–625. <https://doi.org/10.1007/BF02481593>
- Canha RMF, Kuchma DA, El Debs MK, de Souza RA (2014) Numerical analysis of reinforced high strength concrete corbels. *Eng Struct* 74:130–144. <https://doi.org/10.1016/J.ENGSTRUCT.2014.05.014>
- Demir A, İnce Y, Altıok TY (2021) Experimental and numerical investigation of RC beams strengthened with CFRP composites. *J Croat Assoc Civ Eng* 73(06):605–616. <https://doi.org/10.14256/JCE.3051.2020>
- dos Santos LR, de Cardoso H, S, Caldas RB, Grilo LF, (2020) Finite element model for bolted shear connectors in concrete-filled steel tubular columns. *Eng Struct*. <https://doi.org/10.1016/J.ENGSTRUCT.2019.109863>
- El-Maaddawy TA, Sherif E-SI (2014) Response of concrete corbels reinforced with internal steel rebars and external composite sheets: experimental testing and finite element modeling. *J Compos Constr*. [https://doi.org/10.1061/\(asce\)cc.1943-5614.0000403](https://doi.org/10.1061/(asce)cc.1943-5614.0000403)
- El-Refaie SA, Ashour AF, Garrity SW (2003) Sagging and hogging strengthening of continuous reinforced concrete beams using CFRP sheets. *ACI Struct J* 100:446–453
- Fattuhi NI (1990) Strength of SFRC corbels subjected to vertical load. *J Struct Eng* 116:701–718. [https://doi.org/10.1061/\(ASCE\)0733-9445\(1990\)116:3\(701\)](https://doi.org/10.1061/(ASCE)0733-9445(1990)116:3(701))
- Fattuhi NI (1994) Strength of FRC corbels in flexure. *J Struct Eng* 120:360–377. [https://doi.org/10.1061/\(ASCE\)0733-9445\(1994\)120:2\(360\)](https://doi.org/10.1061/(ASCE)0733-9445(1994)120:2(360))
- Fattuhi NI, Hughes BP (1989) Ductility of reinforced concrete corbels containing either steel fibers or stirrups. *Structural J* 86:644–651
- Gulsan ME, Cevik A, Mohmmad SH (2021) Crack pattern and failure mode prediction of SFRC corbels: experimental and numerical study. *Comput Concr* 28:507–519. <https://doi.org/10.12989/CAC.2021.28.5.507>
- Hafezolzghorani M, Hejazi F, Vaghei R et al (2017) Simplified damage plasticity model for concrete. *Struct Eng Int* 27:68–78. <https://doi.org/10.2749/101686616X1081>
- Ivanova I, Assih J (2015) Static and dynamic experimental study of strengthened inforced short concrete corbel by using carbon fabrics, crack path in shear zone. *Frat Ed Integrità Strutt* 9:90–98. <https://doi.org/10.3221/IGF-ESIS.34.09>
- Ivanova I, Assih J, Li A et al (2015) Experimental investigation into strengthened short reinforced concrete corbels by bonding carbon fiber fabrics. *J Adhes Sci Technol* 29:2176–2189. <https://doi.org/10.1080/01694243.2015.1060060>
- Ivanova I, Assih J, Dontchev D (2019) Repairing of short reinforced concrete corbel by bonding composite material under continuous load. *framcos.org*. <https://doi.org/10.21012/FC10.235590>
- Ivanova I, Assih J, Dontchev D (2020) Influence of anchorage length of composite fabrics and bonded surface on the strengthened short reinforced concrete corbel by bonding CFRF. *Eur J Environ Civ Eng* 24:1993–2009. <https://doi.org/10.1080/19648189.2018.1498395>
- Jafarian N, Mostofinejad D, Naderi A (2020) Effects of FRP grids on punching shear behavior of reinforced concrete slabs. *Structures* 28:2523–2536. <https://doi.org/10.1016/J.ISTRUC.2020.10.061>
- Jawad D, Abdul-Hasan M (2018) Nonlinear Finite Element Analysis of Reinforced Concrete Brackets. *Int J Sci Eng Res*
- Maghsoudi AA, Bengar HA (2011) Acceptable lower bound of the ductility index and serviceability state of RC continuous beams strengthened with CFRP sheets. *Scientia Iranica* 18(1):36–44
- Mattock AH, Chen KC, Soongswang K (1976) The behavior of reinforced concrete corbels. *PCI J* 21(2):52–77. <https://doi.org/10.15554/pci.03011976.52.77>
- Mhalhal Jasim M, Manal Alawsi A, Thaar Al-Gasham S (2021) Decays in strength, ductility, stiffness, and toughness of RC corbels due to fire exposure. In: IOP conference series: materials science and engineering. vol 1058, No. 1, IOP Publishing 2021
- Mohammad AKQ, Al-Shamaa MFK (2018) Experimental study of behaviour of reactive powder concrete strengthening by NSM-CFRP corbels. *Civ Eng J* 4(5):980. <https://doi.org/10.28991/cej-0309150>
- Mohammed A, Hassan G, Mohammed AA, Hassan GB (2012) Prediction of load capacity of reinforced concrete corbels strengthened with CFRP Sheets effect of crude oil on performance of RC columns wrapped with CFRP in Kurdistan environment view project ferrocement beam view project prediction of load capacity of
- Njeman AM, Mahmood AS (2018) Ductility and toughness of unsymmetrical CFRP strengthening of reinforced concrete beams. *Iraqi J Civ Eng* 12(1):10–25. <https://doi.org/10.37650/ijce.2018.142404>
- Ozden S, Atalay HM (2011) Strengthening of reinforced concrete corbels with GFRP overlays. *Sci Eng Compos Mater* 18:69–77. <https://doi.org/10.1515/SECM.2011.009>
- Rafati A, Razavi S (2016) Finite element analysis of reinforced RC bracket using CFRP plates. *J Solid Mech* 8:734–743
- Ridha MMS, Al-Shafi'i Hasan NTHMM (2017) Ultra-high performance steel fibers concrete corbels: experimental investigation. *Case Stud Constr Mater* 7:180–190. <https://doi.org/10.1016/J.CSCM.2017.07.004>
- Saleh I, Faleh S (2022) Effects of fiber type and shape on the shear behavior of reinforced concrete corbels without hoop re-bars. *Civ Eng J* 8(3):519–530. <https://doi.org/10.28991/CEJ-2022-08-03-08>
- Saleh A, Fathy A, Farouk A, Nasser M (2019) Performance of steel fiber reinforced concrete corbels. *Int Res J Innov Eng Technol* 3:22–27
- Sayhood EK, Hassan QAM, Layla AGh, Yassin LA (2016) Enhancement in the load-carrying capacity of reinforced concrete corbels strengthened with cfrp strips under monotonic or repeated loads. *Eng Technol J* 34(14):2705–2719. <https://doi.org/10.30684/etj.34.14A.14>

- Spadea G, Bencardino F, Swamy RN (1997) Strengthening and upgrading structures with bonded CFRP sheets design aspects for structural integrity proc. In: 3rd international symposium on non-metallic (FRP) reinforcement for concrete structures 1 pp 629–36
- Strauss A, Mordini A, Bergmeister K (2006) Nonlinear finite element analysis of reinforced concrete corbels at both deterministic and probabilistic levels. *Comput Concr an Int J* 3:123–144. <https://doi.org/10.12989/cac.2006.3.2/3.123>
- Wahalathantri B (2011) DT-P of the, 2011] U A material model for flexural crack simulation in reinforced concrete elements using ABAQUS. *eprints.qut.edu.au* 260–264
- Yun YM, Lee Y (2021) Strengths of struts and nodal zones for strut-and-tie model design of reinforced concrete corbels. *Civ Eng J* 7(8):1275–1289. <https://doi.org/10.28991/cej-2021-03091725>

Springer Nature or its licensor (e.g. a society or other partner) holds exclusive rights to this article under a publishing agreement with the author(s) or other rightsholder(s); author self-archiving of the accepted manuscript version of this article is solely governed by the terms of such publishing agreement and applicable law.